frontiers | Frontiers in Marine Science

TYPE Original Research
PUBLISHED 29 September 2022
DOI 10.3389/fmars.2022.979137

OPEN ACCESS

EDITED BY
Terry Eugene Whitledge,
Retired, Fairbanks, AK, United States

REVIEWED BY
Omid Safari,
Ferdowsi University of Mashhad, Iran
Zorica Tomičić,
Institute of Food Technology,
University of Novi Sad, Serbia

*CORRESPONDENCE
Sang Heon Lee
sanglee@pusan.ac.kr

SPECIALTY SECTION
This article was submitted to Marine Biogeochemistry, a section of the journal Frontiers in Marine Science

RECEIVED 27 June 2022
ACCEPTED 15 September 2022
PUBLISHED 29 September 2022

CITATION
Jo N, Youn S-H, Joo H, Jang HK, Kim Y, Park S, Kim J, Kim K, Kang JJ and Lee SH (2022) Seasonal variations in biochemical (biomolecular and amino acid) compositions and protein quality of particulate organic matter in the Southwestern East/Japan Sea. *Front. Mar. Sci.* 9:979137. doi: 10.3389/fmars.2022.979137

Seasonal variations in biochemical (biomolecular and amino acid) compositions and protein quality of particulate organic matter in the Southwestern East/Japan Sea

Naeun Jo[1], Seok-Hyun Youn[2], HuiTae Joo[2], Hyo Keun Jang[1], Yejin Kim[1], Sanghoon Park[1], Jaesoon Kim[1], Kwanwoo Kim[1], Jae Joong Kang[2] and Sang Heon Lee[1]*

[1]Department of Oceanography, Pusan National University, Busan, South Korea, [2]Oceanic Climate and Ecology Research Division, National Institute of Fisheries Science, Busan, South Korea

The biochemical compositions of marine particulate organic matter (POM) can provide significant information to understanding the physiological conditions of phytoplankton and food quality for their potential consumers. We investigated the seasonal variations in biomolecular and amino acid (AA) compositions of the bulk POM in the southwestern East/Japan Sea from four different sampling months (February, April, August, and October) in 2018. In terms of the biomolecular composition of the POM, overall carbohydrates (CHO) were predominant among three biomolecules accounting for 48.6% followed by lipids (LIP; 35.5%) and proteins (PRT; 15.9%) in the East/Japan Sea. However, markedly seasonal differences in the biomolecular composition of POM were found from February to October, which could be due to seasonally different conditions favorable to phytoplankton growth. Dominant AA constituents to trace POM lability were glycine (GLY), alanine (ALA), and glutamic acid (GLU), suggesting that our POM was the mixtures of decomposing and fresher materials. Furthermore, the significantly negative correlation between the proportion of total essential amino acids (EAAs) and PRT composition ($r = -0.627$, $p < 0.01$) was probably reflected by nutrient availability to phytoplankton partitioning EAAs or non-essential AAs (NEAAs). The different biomolecular compounds under un- or favorable growth conditions for phytoplankton could determine the nutritional quality of POM as potential prey as well as degradation status of POM. Therefore, the biochemical compositions of phytoplankton-originated POM hold important ecological implications in various marine ecosystems under ongoing climate changes.

KEYWORDS

particulate organic matter, phytoplankton, biomolecular composition, amino acid composition, essential amino acids, food quality, East/Japan Sea

Introduction

Marine particulate organic matter (POM) mostly derived from phytoplankton is the foundation of marine food webs and plays a key role in primary producer-herbivore interactions as a pivotal food source (Dzierzbicka-Głowacka et al., 2010; Andersson et al., 2017). The major biochemical components of POM within a euphotic zone are composed of organic biomolecules such as carbohydrates (CHO), proteins (PRT), and lipids (LIP) that phytoplankton synthesize through photosynthesis by taking up inorganic carbon (Fernández-Reiriz et al., 1989; Geider and La Roche, 2002). Increasing or decreasing their synthesis of individual biomolecules depends on facing environmental conditions (e.g. the availability of light and nutrients, temperature and salinity, and the physiological state of phytoplankton (Geider and La Roche, 2002; Bhavya et al., 2019).

Among these biomolecules, amino acids (AAs) have received considerable attention because of their importance to indicate organic matter degradation (Dauwe and Middelburg, 1998; Dauwe et al., 1999) and PRT quality (Oser, 1959; Mente et al., 2002). AAs are the most labile fraction of bulk POM and those compositional changes can provide information on the degradation state of POM, phytoplankton assemblage composition, and phytoplankton growth phase (Hecky et al., 1973; Kolmakova and Kolmakov, 2019; Shields et al., 2019). On the other hand, essential AAs (EAAs) are considered vital to most herbivores since they cannot synthesize the EAAs by themselves, and therefore the availability of EAAs in their diet can affect consumers' growth and reproduction (Muller-Navarra, 1995; Kleppel et al., 1998; Kolmakova and Kolmakov, 2019).

The East/Japan Sea is a marginal sea located in the northwestern Pacific Ocean that has shown marked seasonal patterns in water properties (Kim et al., 2007). Meanwhile, the East/Japan Sea has been considered to be a highly productive region, especially the southwestern part (Lee et al., 2009; Yoo and Park, 2009; Lee et al., 2014), although nitrogenous nutrients are nearly depleted (Kim et al., 2010). Recently, the East/Japan Sea has undergone dramatic environmental changes in physicochemical properties over recent decades (Jo et al., 2017 and references therein). Several studies reported a drastic increasing trend in sea surface temperature in the East/Japan Sea during summer as well as winter after 2010 (Kim and Kim, 1996; Kim et al., 2001; Han and Lee, 2020). Furthermore, Lee et al. (2014) observed different trends of spring blooms in terms of timing, magnitude, and duration between 1998–2001 and 2008–2011. These changes in marine environmental conditions as climate stressors could have influenced cell physiological processes and in turn biochemical compositions of phytoplankton (Kremp et al., 2012; Bhavya et al., 2019). Therefore, biochemical compositions could provide a clue to understanding the physiological response of the phytoplankton community to the ongoing environmental changes.

Here, the aims of the paper were to (1) investigate the seasonal variability in the biochemical (biomolecular and AA) compositions of bulk POM, and (2) determine major controlling factors for the changes in these compositions and PRT quality in the southwestern East/Japan Sea.

Materials and methods

Study area and sampling

The field survey was conducted at each 9-10 stations as a part of the serial oceanographic observation project of the National Institute of Fisheries Science (NIFS) in the southwestern part of the East/Japan Sea on the research vessel Tamgu 3 during four periods (February, April, August, and October 2018) (Figure 1 and Table 1). We chose geographically dispersed 9-10 stations for providing a representative data covering the southwestern East/Japan Sea (Figure 1). For seasonal analyses, these four sampling months were used to represent late winter, spring, summer, and autumn, respectively. The vertical temperature and salinity profiles were obtained with a conductivity-temperature-depth (CTD) recorder (SeaBird Electronics Inc, SBE 911 plus). In order to estimate the euphotic zone depth at which photosynthetic available radiation (PAR) is 1% of its surface value, the secchi disk was used to measure the secchi depth (Kirk, 1985). Then, light penetration depths were calculated by the light attenuation coefficient of PAR estimated from the secchi depth (Kirk, 1985; Padial and Thomaz, 2008). Seawater samples for biological and chemical analyses were collected at three light depths (representing 100, 30, and 1% of the light penetration depths which were estimated by Secchi disk) using 10 L Niskin bottles equipped with CTD/rosette sampler.

Analyses of major dissolved inorganic nutrients and photosynthetic pigments

Seawater samples for analyses of major dissolved inorganic nutrients (phosphate, nitrate + nitrite, ammonium, and silicate) were prefiltered through the Whatman GF/F filter (25 mm, 0.7 μm pore) on board and immediately frozen at -20°C for later processing. Nutrient concentrations were determined photometrically following the standard procedure according to the 'QuAAtro Applications' using an automatic analyzer (QuAAtro, Seal Analytical, Norderstedt, Germany)at the laboratory in the NIFS.

Samples for determination of total chlorophyll-*a* (chl-*a*) concentration were filtered onto 25 mm GF/F filter papers (Whatman, 0.7 μm pore) and extracted in 90% acetone in the refrigerator at 4°C for 24 hours (Parsons et al., 1984). The chl-*a*

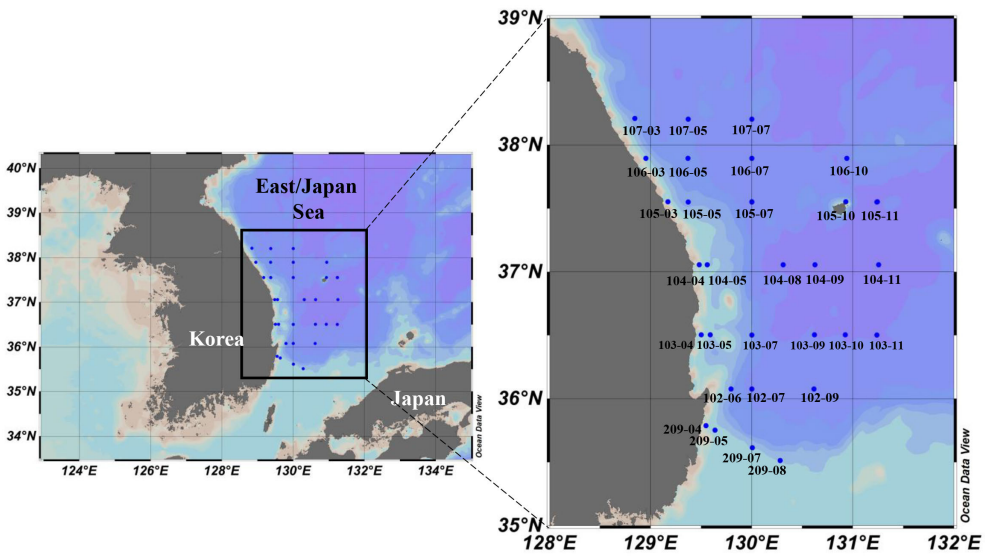

FIGURE 1
Study region in the southwestern East/Japan Sea showing the location of sampling stations.

concentration was calculated by measuring the fluorescence using the pre-calibrated 10-AU fluorometer (Turner Designs, USA). Measurements of size-fractionated chl-*a* concentration were performed on water samples serially passed through a 20 µm-Polycarbonate Track Etched (PCTE) membrane filter (GVS, 47mm), a 2 µm-PCTE membrane filter (Whatman, 47mm), and a 0.7 µm-GF/F filters (Whatman, 47mm). The size-fractionated chl-*a* fluorescence was measured according to the same analysis procedure of total chl-*a*.

Photosynthetic pigments were extracted from frozen filters (1 L or 2 L of seawater, by 47 mm Whatman GF/F filters of pore size of 0.7 µm) in 5mL of 100% acetone (LiChrosolv, Merck, HPLC gradient grade) with 100 µL canthaxanthin (Sigma-Aldrich, USA) as an internal standard and stored in the refrigerator at 4°C for 24 hours as described in a previous study (Kim et al., 2020). The filtrates were filtered by using polytetrafluoroethylene (PTFE)syringe filters of pore size 0.2 µm (Advantec, Japan). For quantifying pigment concentrations, the samples were analyzed using a high-performance liquid chromatography system (HPLC; Agilent Infinity 1260, Santa Clara, CA, USA) following the method of Zapata et al. (2000) with slight modifications (Kim et al., 2020). The pigments used for phytoplankton taxonomic identification were entered into the CHEMTAX program, which allowed estimating the contribution of the main phytoplankton classes based on the ratio of each diagnostic pigment to total chl-*a* (Mackey et al., 1996). The detailed analytical procedures were reported in Kim et al. (2020).

Particulate organic carbon, nitrogen, and stable carbon isotopes ($\delta^{13}C$) analyses of POM

Water samples (0.3 L) for POC and PON concentrations were filtered through the Whatman GF/F filter (25 mm, 0.7 µm pore). The filtered samples were immediately frozen and then acidified over fuming Hydrochloric Acid (HCl; Wako, Japan) to eliminate inorganic carbon at the home laboratory. The filters were transferred into tin capsules and then were analyzed for POC, PON contents, and $\delta^{13}C$ using a Finnigan Delta+ XL mass spectrometer (ThermoFinnigan, Bremen, Germany) at the stable isotope laboratory of the University of Alaska Fairbanks, USA.

Biomolecular composition analyses

Seawater samples for biomolecular composition (CHO, PRT, and LIP) of POM were collected from three light depths (100, 30, and 1%). Each sample (0.5 L) was filtered through a 47mm Whatman GF/F filter (0.7 µm pore) and the filtered samples were immediately frozen (- 80 °C). In the laboratory, The UV-visible spectrophotometric (Hitachi UH-5300, Japan) methods were used to measure each biomolecular concentration. The phenol-sulfuric method proposed by Dubois et al. (1956) was used to quantify the total CHO of POM. The total PRT content was determined according to Lowry et al. (1951). The total LIP content was extracted according to the method of Bligh

TABLE 1 Information on sampling stations, associated environmental variables, and concentrations of major inorganic nutrients during this study.

Month	station	Latitude (°N)	Longitude (°E)	Light depth (%)	Sampling depth (m)	Zm (m)	Water Temperature (°C)	Salinity	PO_4 (μM)	NO_2 +NO_3 (μM)	NH_4 (μM)	SIO_2 (μM)	N/P ratio (molar: molar)
Feb.	103-07	36.50	130.00	100	0	87	10.19	34.39	0.45	7.23	0.47	10.11	17.2
				30	14		10.19	34.39	0.44	6.75	0.34	10.12	16.1
				1	54		10.18	34.39	0.42	6.84	0.32	9.47	16.9
	103-11	36.50	131.24	100	0	33	10.99	34.44	0.35	5.59	0.32	9.64	16.7
				30	12		10.92	34.44	0.34	5.26	0.38	9.78	16.4
				1	46		9.73	34.32	0.34	6.87	0.33	10.02	21.4
	105-05	37.55	129.37	100	0	30	8.20	34.29	0.52	8.13	0.41	11.22	16.3
				30	13		8.19	34.28	0.40	7.30	0.31	6.08	18.9
				1	51		4.55	34.06	0.87	12.74	0.60	16.62	15.3
	105-07	37.55	130.00	100	0	123	9.51	34.28	0.36	6.95	0.32	8.43	20.3
				30	14		9.46	34.28	0.33	6.36	0.25	5.27	20.1
				1	54		9.34	34.27	0.40	6.83	0.32	8.29	17.8
	105-11	37.55	131.24	100	0	135	8.89	34.28	0.43	6.73	0.21	8.14	16.3
				30	14		8.95	34.23	0.41	6.54	0.40	8.20	17.0
				1	54		8.94	34.23	0.42	7.28	0.66	8.14	18.8
	107-05	38.20	129.37	100	0	27	8.80	34.21	0.43	7.04	0.89	8.67	18.6
				30	11		8.84	34.25	0.35	6.79	0.88	6.35	22.0
				1	43		7.18	34.24	0.48	6.79	0.30	9.87	14.8
	107-07	38.20	130.00	100	0	190	8.86	34.20	0.39	6.51	0.01	8.90	16.9
				30	11		8.84	34.17	0.43	6.48	0.03	8.74	15.3
				1	43		8.85	34.17	0.42	6.53	0.02	8.39	15.8
	209-05	35.75	129.64	100	0	51	11.68	34.45	0.47	6.74	0.37	11.33	15.0
				30	14		11.68	34.45	0.46	6.81	0.33	11.31	15.5
				1	54		10.67	34.40	0.56	8.16	0.34	13.09	15.2
	209-08	35.51	130.28	100	0	49	12.73	34.55	0.37	5.26	0.28	11.84	14.8
				30	16		12.67	34.54	0.40	5.35	0.28	11.94	14.1
				1	60		12.09	34.51	0.44	5.22	0.20	12.32	12.2
Apr.	102-06	36.08	129.80	100	0	54	14.65	34.57	0.20	0.83	1.52	4.97	11.9
				30	11		14.56	34.58	0.17	0.94	1.46	3.62	14.5
				1	43		14.40	34.57	0.23	3.02	2.02	4.72	22.3
	103-04	36.51	129.50	100	0	26	12.52	34.35	0.11	0.61	0.25	4.06	8.0
				30	4		12.52	34.34	0.09	0.61	0.28	2.31	10.2
				1	16		12.51	34.35	0.13	0.97	0.30	5.87	10.0
	103-10	36.51	130.93	100	0	11	12.66	34.45	0.06	0.40	0.26	3.14	10.5
				30	6		12.66	34.45	0.07	0.41	0.26	3.06	9.9
				1	24		11.23	34.36	0.13	1.83	0.43	5.55	17.5
	104-05	37.06	129.56	100	0	37	13.52	34.50	0.14	1.50	1.55	3.27	21.9
				30	7		13.51	34.49	0.14	1.65	1.35	6.26	21.3
				1	27		13.50	34.49	0.16	1.81	1.45	3.33	20.0
	104-09	37.06	130.63	100	0	34	11.23	34.39	0.17	2.56	1.63	6.48	24.0
				30	7		11.22	34.39	0.18	2.55	1.61	4.14	23.2
				1	27		10.91	34.39	0.16	3.29	1.33	3.99	29.5
	105-10	37.55	130.93	100	0	48	11.47	34.44	0.22	2.74	0.33	6.71	13.8
				30	6		11.46	34.44	0.16	2.73	0.42	4.69	20.2
				1	24		11.28	34.44	0.19	2.94	0.36	6.74	17.8
	106-03	37.90	128.95	100	0	31	12.20	34.44	0.12	1.95	1.46	3.62	28.6
				30	7		12.21	34.45	0.15	2.22	1.55	4.00	24.6

(Continued)

TABLE 1 Continued

Month	station	Latitude (°N)	Longitude (°E)	Light depth (%)	Sampling depth (m)	Zm (m)	Water Temperature (°C)	Salinity	PO_4 (μM)	NO_2 +NO_3 (μM)	NH_4 (μM)	SIO_2 (μM)	N/P ratio (molar: molar)
				1	27		12.21	34.45	0.14	2.09	1.40	3.77	25.2
	106-10	37.90	130.94	100	0	32	10.00	34.33	0.12	1.49	1.31	3.29	23.8
				30	10		9.97	34.33	0.13	2.47	1.38	3.71	28.7
				1	38		8.24	34.24	0.28	4.48	1.67	4.24	21.7
	107-07	38.20	130.00	100	0	29	10.93	34.44	0.17	3.71	0.25	2.89	23.4
				30	14		10.86	34.40	0.28	3.76	0.27	3.99	14.6
				1	30		10.16	34.35	0.19	3.62	0.25	4.08	20.0
	209-07	35.61	130.01	100	0	60	15.35	34.58	0.16	1.85	0.15	5.25	12.4
				30	6		15.35	34.58	0.17	1.88	0.15	6.56	12.0
				1	22		15.36	34.58	0.18	1.86	0.19	7.52	11.6
Aug	102-09	36.08	130.62	100	0	23	26.65	32.76	0.14	0.14	0.52	5.23	4.9
				30	16		26.63	32.77	0.12	0.09	N.D.	3.77	N.D.
				1	60		17.47	33.31	0.35	5.74	0.66	8.22	18.4
	103-09	36.51	130.62	100	0	9	26.02	33.27	0.16	0.19	0.24	4.95	2.7
				30	17		24.73	33.33	0.17	0.14	0.24	6.15	2.2
				1	65		16.41	34.21	0.64	9.74	0.24	14.16	15.5
	104-04	37.06	129.48	100	0	19	26.34	33.19	0.14	0.19	0.51	4.11	5.1
				30	14		26.30	33.20	0.14	1.90	0.38	3.96	16.5
				1	54		15.69	34.21	0.57	10.48	0.66	13.40	19.4
	104-11	37.06	131.26	100	0	9	25.19	33.15	0.15	0.05	0.53	4.26	3.9
				30	14		24.91	33.33	0.13	0.09	0.76	4.16	6.4
				1	54		9.34	34.23	0.46	8.43	0.66	10.02	19.7
	105-07	37.55	130.00	100	0	21	27.45	33.00	0.13	0.10	0.28	3.15	3.0
				30	16		27.55	32.94	0.13	0.09	0.29	2.95	3.0
				1	60		14.72	34.27	0.51	11.46	0.25	9.69	23.1
	105-11	37.55	131.24	100	0	12	26.56	33.08	0.08	0.35	0.26	3.83	7.9
				30	16		21.38	33.49	0.06	0.12	0.32	2.97	6.9
				1	60		9.62	34.30	0.54	8.68	0.29	11.40	16.7
	106-05	37.90	129.37	100	0	9	25.48	33.05	0.09	0.17	0.60	3.88	8.5
				30	12		17.10	33.67	0.07	0.21	0.39	4.54	8.4
				1	46		6.23	34.16	0.54	9.76	0.48	8.19	19.1
	107-03	38.21	128.84	100	0	6	27.08	32.92	0.07	0.37	0.53	0.89	12.7
				30	10		23.57	33.47	0.10	0.32	0.45	1.60	7.4
				1	30		6.09	33.98	0.11	0.78	0.48	2.85	11.7
	107-07	38.20	130.00	100	0	7	29.15	32.23	0.07	0.14	0.40	0.70	7.9
				30	13		22.98	32.82	0.08	0.17	0.37	1.61	7.0
				1	49		14.83	34.30	0.66	10.74	0.36	14.84	16.8
	209-07	35.61	130.01	100	0	17	26.54	32.44	0.11	0.15	0.34	6.04	4.5
				30	16		26.85	32.35	0.11	0.37	0.25	5.89	5.8
				1	66		14.22	34.15	0.69	11.60	0.28	17.09	17.2
Oct.	102-07	36.08	130.00	100	0	40	21.65	33.96	0.13	1.72	0.74	1.60	18.6
				30	10		21.66	33.96	0.11	1.61	0.57	1.41	19.1
				1	38		21.70	34.03	0.14	1.71	0.70	1.70	17.1
	103-05	36.51	129.59	100	0	30	20.25	33.55	0.08	1.81	0.46	2.41	27.1
				30	10		20.22	33.55	0.12	1.80	0.44	3.20	18.6
				1	38		13.09	34.36	0.82	6.40	0.63	13.97	8.6
	103-09	36.51	130.62	100	0	36	20.36	33.45	0.08	2.38	0.34	2.41	32.5

(Continued)

TABLE 1 Continued

Month	station	Latitude (°N)	Longitude (°E)	Light depth (%)	Sampling depth (m)	Zm (m)	Water Temperature (°C)	Salinity	PO_4 (μM)	NO_2 +NO_3 (μM)	NH_4 (μM)	SIO_2 (μM)	N/P ratio (molar: molar)
				30	9		20.31	33.43	0.10	2.19	0.62	2.26	28.6
				1	35		20.27	33.45	0.26	4.29	0.66	4.52	18.8
	104-08	37.06	130.31	100	0	36	18.56	33.26	0.23	1.60	1.27	3.17	12.3
				30	7		18.57	33.27	0.24	1.79	0.87	3.43	11.0
				1	27		18.42	33.25	0.08	1.60	0.65	2.49	27.4
	105-03	37.55	129.17	100	0	26	18.88	33.26	0.08	0.12	0.61	2.39	9.6
				30	7		18.87	33.27	0.07	0.85	0.58	2.50	19.2
				1	27		18.49	33.42	0.11	1.04	0.54	3.85	13.8
	105-11	37.55	131.24	100	0	61	20.11	33.56	0.05	0.94	0.49	1.66	25.9
				30	8		20.10	33.55	0.06	0.96	0.58	1.07	25.1
				1	30		19.99	33.54	0.06	0.92	0.37	1.26	22.1
	106-07	37.90	130.00	100	0	39	19.54	33.27	0.25	0.40	0.67	5.32	4.3
				30	12		19.52	33.25	0.16	0.40	0.67	3.56	6.8
				1	46		17.06	33.96	0.26	5.87	0.61	6.08	24.5
	107-03	38.21	128.84	100	0	14	17.67	33.33	0.08	0.08	0.17	0.86	3.0
				30	8		17.66	33.33	0.07	0.27	0.17	0.87	6.4
				1	30		7.55	34.16	0.98	14.02	0.14	18.69	14.5
	107-07	38.20	130.00	100	0	37	19.69	33.22	0.08	0.31	0.18	2.02	6.5
				30	12		19.55	33.22	0.05	0.28	0.24	1.66	10.5
				1	46		16.32	34.00	0.59	10.19	0.14	12.16	17.5
	209-04	35.79	129.55	100	0	60	20.90	33.94	0.25	3.29	0.77	4.02	16.5
				30	6		20.92	33.96	0.25	3.21	0.77	3.91	16.2
				1	22		20.52	33.95	0.25	3.28	0.72	3.79	16.0

Z_m, Mixed layer depth, PO_4, Phosphate, NO_2+NO_3, Nitrate+Nitrite, NH_4: ammonium, SiO_2: Silicate, N.D., No data.

and Dyer (1959) and Marsh and Weinstein (1966) with minor modifications. More detailed analytical procedures and calibration methods are explained in Bhavya et al. (2019).

AA composition analysis and degradation index

Water samples for total particulate hydrolyzable amino acids (PAA) analysis were collected from different three-light depths (100, 30, and 1%). Seawater (1 L) from each station was filtered through 47 mm GF/F filters (Whatman, 0.7 μm pore) aboard and frozen immediately at -80 °C until analysis. The composition of PAA was determined by HPLC after HCl hydrolysis and ortho-phthalaldehyde (OPA) and 9-fluorenylmethyl chloroformate (FMOC) (Agilent Technologies, Santa Clara, CA, USA) derivatization according to the procedure in Bartolomeo and Maisano (2006) and Agilent Application note (Henderson et al., 2000). More details on the calibration method and sample measurements are described in our previous study (Jo et al., 2021). PAA compositions were determined for the following 16 L-AAs (Agilent Technologies, Santa Clara, CA, USA): Aspartic acid (ASP), Glutamic acid (GLU), Serine (SER), Histidine (HIS), Glycine (GLY), Threonine (THR), Arginine (ARG), Alanine (ALA), Tyrosine (TYR), Cystine (CY2), Valine (VAL), Methionine (MET), Phenylalanine (PHE), Isoleucine (ILE), Leucine (LEU), Lysine (LYS). The concentration of each AA was expressed as a mole percentage (mol%) of PAA. Additionally, individual AAs were grouped into nine essential (EAA: histidine, threonine, arginine, valine, methionine, phenylalanine, isoleucine, leucine, and lysine) and six non-essential (NEAA: aspartic acid, glutamic acid, serine, glycine, alanine, and tyrosine) ones.

The mole percentages (mol%) of PAA were used to calculate the degradation index (DI) proposed by Dauwe et al. (1999). For the calculation of DI from PAA in this study, mole percentages of the AAs were standardized using averages, and standard deviations and multiplied with factor coefficients as given in Dauwe et al. (1999) according to the formula:

$$DI = \sum_i \left[\frac{var_i - AVGvar_i}{STDvar_i}\right] \times fac \cdot coef_i$$

where var_i is the mol% of the individual AA, $AVGvar_i$ and $STDvar_i$ are the mean and standard deviation of the AA mol% in our data set and $fac{\cdot}coef_i$ is the factor coefficient for each AA in Dauwe et al. (1999).

Statistical analysis

The concentrations of total chl-*a*, POC/N, and biomolecular compounds used for presenting the spatial and temporal variations are expressed as depth-weighted averages which can be obtained by dividing the trapezoidal integration of measured values for each biochemical parameter by the maximum sampling depth (Crosbie and Furnas, 2001). We utilized the depth-weighted average because it assumed homogeneity within the euphotic water column, which made it better suited for the distributional patterns of our samples (Wei et al., 2020). The depth-weighted average equation was calculated following this formula (Wei et al., 2020):

$$A = \left[\sum_{i=1}^{n-1} \frac{A_i + A_{i+1}}{2} \times (D_{i+1} - D_i)\right] / D$$

where A is the mean value of each biochemical parameter; A_i is the concentration of each biochemical parameter at layer i (m); Di is the depth at sampling layer i (m); D is the depth of the maximum sampling layer (m), and n is the number of sampling layers.

To explore significant differences between the two or more than two variables were performed using the t-test or analysis of variance (ANOVA) with the *post hoc* test (Scheffe's test). Pearson's correlation coefficients were used to examine the significant correlation between variables. In all statistical analyses, the statistical significance of the results was accepted at p values<0.05. Statistical analyses were achieved using an IBM SPSS statistics software package 25.0 (IBM software, Chicago, IL, USA).

To investigate which environmental variables could best describe the variability in biochemical compositions (biomolecular and AA compositions) of POM, a multivariate form of direct gradient analysis (Redundancy Analysis, hereafter RDA) was performed using the CANOCO software 4.5 (Biometris, Wageningen, The Netherlands) for Windows (ter Braak and Šmilauer, 2002). Prior to RDA, a detrended correspondence analysis (DCA) was executed to ensure the applicability of the linear RDA. DCA result showed a gradient length of the first axis smaller than 3 standard deviations, suggesting that redundancy analysis (RDA) was the appropriate method for our data (Ramette, 2007). The Monte Carlo permutation test with 999 permutations was conducted to evaluate the statistical significance of the first ordination axis and the first four canonical axes together.

Results

Hydrological and chemical properties

Depth profiles of water temperature, salinity, and concentrations of major dissolved inorganic nutrients during the four cruises are represented in Table 1. Overall, when mixed layer depth is located below the euphotic zone, the vertical distributions of temperature and salinity within the euphotic zone were rather homogenous during this study. By contrast, when mixed layer depth was shallower than 1% light depth, temperature values at 1% light depth were lower than those in the upper layer (100 and 30% light depths). The ranges of temperature within the euphotic water column in February, April, August, and October were 4.55 – 12.73°C, 8.24 – 15.36 °C, 6.09 – 29.15°C, and 7.55 – 21.70°C, respectively (Table 1). The salinity showed low variability throughout the study period ranging from 32.23 to 34.58 with the highest values in April (mean ± S.D. = 34.44 ± 0.09) and the lowest values in August (mean ± S.D. = 32.23 ± 0.63) (Table 1).

The major dissolved inorganic nutrients (phosphate, nitrate + nitrite, ammonium, and silicate) also showed seasonal variations (Table 1). In general, February was characterized by higher concentrations of phosphate, nitrate + nitrite, and silicate than other periods (Table 1). The highest variability among the sampling stations in ammonium concentrations was observed in April, with the higher values (> 1.3 μM) throughout the euphotic water column collected from some stations (st.102-06, 104-05, 104-09, 106-03, and 106-10). In August and October, phosphate, nitrate + nitrite, and silicate at the 1% light depth had even higher values than those in the upper layer (100 and 30% light depths). The phosphate concentrations within the euphotic zone were 0.33 – 0.87 μM in February, 0.06 – 0.28 μM in April, 0.06 – 0.69 μM in August, and 0.05 – 0.98 μM in October (Table 1). The concentrations of nitrate + nitrite in February showed higher values (5.22 – 12.74 μM), whereas those in the upper layer in August almost were depleted. The ammonium concentrations during this study were mostly low (< 1 μM) except above-mentioned stations in April. The ranges of silicate concentrations within the euphotic zone in this study were 5.27 – 16.62 μM in February, 2.31 – 7.52 μM in April, 0.70 – 17.09 μM in August, and 0.86 – 18.69 μM in October, respectively (Table 1). Dissolved inorganic nitrogen (nitrate + nitrite + ammonium; N) to phosphorus (P) ratio (N/P ratio) within the euphotic layer ranged from 12.2 to 22.0 in February (mean ± S.D. = 16.9 ± 2.3), from 8.0 to 29.5 in April (mean ± S.D. = 18.4 ± 6.4), from 2.2 to 23.1 in August (mean ± S.D. = 10.4 ± 6.3), and from 3.0 to 32.5 in October (mean ± S.D. = 16.6 ± 7.8) (Table 1).

Phytoplankton biomass and community structure

Overall, the phytoplankton biomass represented by depth-weighted average concentrations of total chl-*a* from surface to 1% light depth varied seasonally from 0.1 to 3.0 μg L^{-1}, with higher values (mean ± S.D. = 1.9 ± 0.7 μg L^{-1}) in April and lower values (mean ± S.D. = 0.2 ± 0.1 μg L^{-1}) in August. The depth-weighted average total chl-*a* concentrations within the euphotic zone ranged from 0.4 to 2.0 μg L^{-1} in February, from 1.1 to 3.0 μg L^{-1} in April, from 0. 1 to 0.4 μg L^{-1} in August, and 0.4 – 2.1 μg L^{-1} in October (Table 2).

The mean contributions of different size-fractionated chl-*a* (> 20 μm, 2 – 20 μm, and 0.7 – 2 μm) profiles during this study were variable among the sampling stations except for August (Table 2). In this study, the relative contributions of large (>20 μm), middle (2 – 20 μm), and small-sized (0.7 – 2 μm) fractions to the total phytoplankton chl-*a* concentrations were 4.0 – 72.9, 12.0 – 41.8, and 13.4 – 68.6%, respectively (Table 2). In August, the relative contributions of size-fractionated chl-*a* indicate small-size class (0.7 – 2 μm) to be the major contributor (mean ± S.D = 56.2 ± 13.0%) except st. 209-07 (Table 2). By comparison, for the other three months (February, April, and October), changes in size groups of phytoplankton were highly dynamic and the relative dominances of large-sized or small-sized phytoplankton appeared across the study region (Table 2).

The relative contribution of different phytoplankton groups to total chl-*a* estimated by CHEMTAX varied also largely across the sampling stations during our study (Table 2). However, diatoms had the greatest average contribution to total chl-*a* (mean ± S.D = 36.3 ± 22.5%) throughout this study period. In February, cryptophytes and prasinophytes had relatively higher contributions where diatoms were not predominated. Dinoflagellates appeared peculiarly with a maximum value of 25.8% in April (Table 2). The contribution of cyanobacteria increased in August and October (mean ± S.D = 28.5 ± 17.5% and 13.9 ± 12.3%, respectively) along with a higher proportion of small-sized class (0.7 – 2 μm) (Table 2).

Particulate organic carbon, nitrogen, and stable carbon isotopes ($\delta^{13}C$) of POM

The analytical results of the parameters POC, PON, C/N ratio, POC/Chl-*a* ratio, and $\delta^{13}C$ of bulk POM are displayed in Table 3. The depth-weighted average POC and PN concentrations of POM varied over a wide range during this study (Table 3). The euphotic depth-averaged C/N molar ratios showed wide variability depending on the seasons, ranging from 5.4 to 15.8 with the highest values in August (range: 10.8 – 15.8) and lower values in April and October (range: 5.9 – 8.5, 5.4 – 9.3, respectively) (Table 3). There was a wide range of variability in the mean POC/Chl-*a* ratio within the euphotic zone among sampling months, ranging from 66.6 to 299.3 (February), 58.9 to 131.3 (April), 532.7 to 1328.0 (August), and 88.2 to 189.0 (October), respectively (Table 3). The averages of the POC/Chl-*a* ratio in August were markedly higher than those during other sampling seasons (one-way ANOVA, $p< 0.05$). The $\delta^{13}C$ values of surface POM ranged from -26.3 to -18.8 ‰ with lower variability throughout the study period (Table 3).

Biomolecular composition of POM

The depth-weighted average concentrations and relative proportions of CHO, PRT, LIP, and food material (hereafter FM; i.e., the sum of the CHO, PRT, and LIP concentrations in POM; Danovaro et al., 2000) varied significantly at similar sampling stations depending on the season (Table 4). Taking the entire data set into account, the depth-weighted average concentrations of biomolecules (CHO, PRT, and LIP) ranged from 60.0 to 253.9, from 2.7 to 147.4, and 44.3 to 157.7 μg L^{-1}, respectively (Table 4). The depth-weighted average FM concentration in the total POM in the southwestern East/Japan Sea varied from 130 to 471.8 μg L^{-1} in this study and reached its maximum value in April consistent with the total chl-*a* biomass peak. Indeed, a linear relationship observed between the total FM concentration and the total chl-*a* concentration ($r = 0.783$, $n = 115$, $p< 0.01$) indicates that FM concentrations vary coincidentally with phytoplankton biomass.

The relative proportions of biomolecular components (CHO, PRT, and LIP) in the total POM were averaged from the surface to 1% light depth since there were no statistically significant differences among the three light depths (one-way ANOVA, $p > 0.05$). CHO were the largest contributor to the biomolecular composition of the bulk POM, representing on average 48.6% (S.D = 11.3%) during the study period although the biomolecular composition of POM displayed a remarkable seasonal variability (Table 4 and Figure 2). CHO composition was discovered to be clearly high (46.6 – 69.4%) in February at all the stations, while PRT composition was lower (2.4 – 18.7%) than those of other seasons (Table 4). The contribution of CHO notably decreased (35.2 – 54.5%) whereas PRT showed a distinct increase (20.7 – 32.9%) in April relative to February (Table 4). However, CHO proportion was found to be dominant again in August and contributed approximately > 50% to total biomolecular composition in the total POM (Table 4 and Figure 2). In comparison, the contribution of LIP in October was much higher than that of other months and comprised 38.6 to 57.5% of POM (Table 4 and Figure 2). The ternary diagram illustrated the relative proportions of CHO, PRT, and LIP indicating that the biomolecular composition of bulk POM showed a clear seasonality than their regional variability (Figure 3). Plotting the analyzed samples on this plot were divided into three groups: overwhelmingly predominant CHO proportion in February and April, relatively higher PRT proportion in August, and dominant LIP proportion in October (Figure 3).

Amino acid composition of POM and amino acid indices

The concentrations measured at 14 detected AAs were summed to quantify the total PAA concentrations. The PAA concentrations in bulk POM during the study showed no differences between the three light depths except in October (one-way ANOVA, $p > 0.05$, OCT: one-way ANOVA, $p< 0.05$, $p = 0.011$). The PAA concentrations within the euphotic zone spanned the range from 0.07 to 0.31 μM in February, from 0.27 to 1.71 μM in April, from 0.12 to 0.55 μM in August, and from 0.13 to 0.78 μM in October, respectively (Supplementary Table 1). The high PAA

TABLE 2 Depth-weighted average total chl-*a* concentrations, averaged compositions of different size-fractionated chl-*a* and phytoplankton communities from three light depths in southwestern East/Japan Sea, 2018.

Month	Station	Chl-*a*				Phytoplankton community composition (%)							
		depth-weighted (μg L^{-1})	> 20 μm (%)	2-20 μm (%)	0.7-2 μm (%)	Prasinophytes	Dinofla-gellates	Cryptophytes	Prymnesio-phytes	Pelagophytes	Chlorophytes	Cyanobacteria	Diatoms
FEB.	St.103-07	0.9	38.0	22.7	39.3	16.0	0.0	20.1	2.5	8.4	1.3	0.0	51.7
	St.103-11	2.0	72.9	13.7	13.4	5.5	0.0	11.6	1.9	5.3	0.8	0.1	74.8
	St.105-05	0.4	9.9	39.1	51.0	19.9	0.0	24.2	4.4	9.5	2.0	0.8	39.2
	St.105-07	0.5	17.9	25.0	57.1	25.7	0.0	34.3	6.3	14.1	2.7	0.3	16.6
	St.105-11	0.5	16.8	25.5	57.7	26.7	0.0	34.8	7.2	13.5	1.4	0.0	16.3
	St.107-05	0.8	10.9	34.1	55.0	23.6	0.0	35.9	8.1	17.0	2.0	0.8	12.5
	St.107-07	0.4	45.4	15.3	39.3	11.0	0.0	20.9	5.5	6.8	4.2	0.0	51.5
	St.209-05	0.4	16.1	41.8	42.1	27.3	0.0	23.3	3.7	14.0	2.7	0.0	28.9
	St.209-08	0.8	57.1	20.2	22.7	8.9	0.0	12.7	3.7	13.0	1.7	0.0	59.9
APR.	St.102-06	1.4	60.7	12.0	27.2	21.3	9.8	9.3	7.8	0.0	4.5	11.0	36.3
	St.103-04	2.8	41.7	29.7	28.7	15.8	12.3	3.7	11.2	7.3	2.4	5.4	41.9
	St.103-10	3.0	29.7	30.6	39.7	12.6	8.1	15.4	12.9	10.3	4.5	10.5	25.7
	St.104-05	2.3	21.2	39.0	39.7	27.0	8.7	3.1	17.4	13.0	1.6	4.3	24.8
	St.104-09	2.3	4.0	37.9	58.1	21.3	7.9	18.4	11.8	16.1	4.1	8.0	12.3
	St.105-10	1.5	7.2	37.7	55.1	22.7	10.1	15.6	10.6	13.0	4.1	10.3	13.6
	St.106-03	1.6	20.9	22.9	56.2	23.2	9.1	13.6	9.5	9.5	5.5	11.0	18.6
	St.106-10	1.1	20.2	30.4	49.4	27.0	19.5	8.0	9.8	9.6	2.8	8.5	14.8
	St.107-07	1.1	19.1	32.3	48.6	18.0	25.8	9.2	7.1	20.1	0.1	3.2	16.6
	St.209-07	2.1	50.8	23.6	25.6	35.3	9.5	12.2	11.0	4.8	0.0	1.0	26.2
AUG.	St.102-09	0.2	18.2	17.6	64.2	0.0	3.2	0.3	9.8	7.4	16.2	30.7	32.4
	St.103-09	0.3	13.6	18.2	68.2	0.0	6.0	0.4	12.4	28.8	16.1	28.0	8.2
	St.104-04	0.2	13.2	18.2	68.6	0.0	0.0	0.0	10.5	18.3	18.8	35.0	17.4
	St.104-11	0.2	26.8	20.6	52.6	0.0	0.0	0.2	14.1	0.0	28.8	28.6	28.3
	St.105-07	0.1	17.6	20.7	61.7	0.0	0.0	0.1	1.5	10.7	4.4	66.5	16.8
	St.105-11	0.2	12.4	41.3	46.3	0.1	0.1	8.9	11.7	16.2	8.2	34.3	20.4
	St.106-05	0.4	12.9	32.7	54.4	8.7	0.1	7.0	14.2	11.1	8.0	11.8	39.2
	St.107-03	0.3	14.6	25.1	60.4	7.8	0.0	25.6	12.5	0.0	6.1	10.7	37.2
	St.107-07	0.2	18.1	21.2	60.7	0.0	0.0	6.3	9.8	11.7	8.8	34.9	28.3
	St.209-07	0.3	42.1	33.0	25.0	0.0	5.2	0.0	3.2	0.0	5.4	4.3	81.9
OCT.	St.102-07	1.2	72.3	14.3	13.5	0.0	0.0	3.3	2.9	0.0	5.4	3.4	85.1
	St.103-05	1.1	41.0	32.2	26.8	0.0	0.0	17.3	2.3	0.0	3.1	2.1	75.1

(Continued)

10.3389/fmars.2022.979137

TABLE 2 Continued

Month	Station	Chl-*a*				Phytoplankton community composition (%)							
		depth-weighted (μg L^{-1})	> 20 μm (%)	2-20 μm (%)	0.7-2 μm (%)	Prasinophytes	Dinofla-gellates	Cryptophytes	Prymnesio-phytes	Pelagophytes	Chlorophytes	Cyanobacteria	Diatoms
	St.103-09	0.8	30.7	22.6	46.7	0.0	0.0	14.7	13.0	9.9	7.3	19.0	36.2
	St.104-08	2.1	44.0	23.3	32.7	4.2	0.0	16.9	5.1	2.7	4.6	5.3	61.2
	St.105-03	0.9	40.0	18.8	41.3	7.7	0.0	11.8	6.2	8.1	6.9	14.6	44.7
	St.105-11	0.7	54.2	13.8	32.0	0.0	0.0	9.0	5.4	9.1	7.7	16.8	51.9
	St.106-07	0.4	18.2	15.6	66.2	0.0	0.0	0.3	10.3	20.3	18.7	40.7	9.6
	St.107-03	1.1	54.4	18.2	27.4	0.1	0.0	3.4	1.5	0.0	3.8	6.8	84.4
	St.107-07	0.4	21.9	16.5	61.6	10.3	0.0	0.2	8.6	23.3	16.1	26.2	15.4
	St.209-04	1.2	25.1	31.3	43.6	3.8	0.0	23.1	1.9	0.0	9.3	4.3	57.5

concentrations were observed in April when the maximum total chl-*a* also occurred. Furthermore, PAA concentrations were positively correlated with total chl-*a* and PRT concentrations (r = 0.726 and r = 0.812 for chl-*a* and PRT, respectively, $p< 0.01$, n = 115). Although the seasonal variations were seen in the mean mol fractions of individual AAs in PAA between February and October, the most abundant AAs throughout this study were GLY, GLU, and ALA (Figure 4). Among these AAs, the highest mean mol percentages (>20%) in PAA were only found for GLY (Figure 4). In contrast, the minor constituents of the PAA were LYS, MET, and ILE in most PAA samples. 5 AAs (ASP, GLU, VAL, MET, and ILE) did not show statistically significant changes with the season in this study (Figure 4; one-way ANOVA, $p > 0.05$). Seasonal contributions of a sum of 9 EAAs to total AAs (∑EAA%) in bulk POM are given in Figure 5A. Ranges of ∑EAA% for February, April, August, and October were 45.1 – 56.9, 36.1 – 46.4, 37.1 – 48.9, and 40.4 – 52.3%, respectively (Supplementary Table 1). ∑EAA% was observed significantly higher in February, followed by October and August, and finally April, with significantly lower values (Figure 5A; one-way ANOVA, $p< 0.05$). In contrast, the percentage compositions of total 6 NEAAs (∑NEAA%) from February to October accounted for 43.1 – 54.9, 53.6 – 63.9, 51.1 – 62.9, and 47.7 – 59.6%, respectively (Supplementary Table 1).

The carbon and nitrogen normalized yields of AAs (AA-POC% and AA-PON%) represent the portion of POC and PON contributed by detecting all AAs in each PAA sample (Supplementary Table 1). The PAA contributed between 3.1 and 49.7% of total POC and between 14.3 and 89.3% of total PON in this study (Figures 5B, C, and Supplementary Table 1). Seasonal trends in the AA-POC% and AA-PON% appeared to be similar to PAA concentrations with higher values occurring in April and October (Figures 5B, C).

A less clear trend emerged in the calculated DI values of bulk POM between three light depths (100, 30, and 1%) during the entire sampling period (Supplementary Table 1), but differences in those depending on the season were significant (Figure 5D; one-way ANOVA, $p< 0.05$). DI values for all PAA samples ranged from -1.00 to 1.60, with an average of 0.00 ± 0.46. DI values were comparatively higher in February (mean ± S.D. = 0.30 ± 0.51) compared to other seasons (mean ± S.D. = -0.09 ± 0.52 (April), -0.11 ± 0.41 (August), -0.07 ± 0.29 (October), respectively).

RDA results

The RDA results showed that the cumulative percentage variance of biochemical compositions data of the first four axes was 30% (Table 5). Furthermore, the cumulative percentage variance of biochemical compositions–environment relation explained by the first and second axes was 75.2% (Table 5). There was a strong correlation between biochemical compositions and environmental factors with biochemical

TABLE 3 Depth-weighted average concentrations of POC and PON, the mean ratios of C/N (molar) and POC/Chl-*a*, and δ13C (‰) of particulate organic matter (POM).

Month	Station	depth-weighted average		C/N ratio (molar:molar)	POC/Chl-a ratio	$\delta^{13}C$ (‰)
		POC (μg C L^{-1})	PON (μg N L^{-1})			
FEB.	St.103-07	103.8	14.2	8.9	110.4	-26.3
	St.103-11	134.3	20.3	7.8	66.6	-23.5
	St.105-05	103.1	12.0	10.8	267.6	-25.4
	St.105-07	102.5	12.5	10.2	200.5	-24.3
	St.105-11	110.4	11.7	10.8	220.7	-24.7
	St.107-05	106.2	14.9	8.4	132.2	-25.5
	St.107-07	79.3	8.8	11.0	194.4	-24.7
	St.209-05	122.0	14.7	10.7	299.3	-22.8
	St.209-08	96.9	15.1	7.6	116.8	-23.0
APR.	St.102-06	125.9	24.2	6.5	90.6	-22.5
	St.103-04	183.6	31.4	7.1	65.7	-21.4
	St.103-10	220.5	41.1	6.3	74.6	-22.6
	St.104-05	139.2	26.3	6.2	60.3	-22.9
	St.104-09	135.0	26.7	5.9	58.9	-24.0
	St.105-10	124.2	21.7	6.5	81.2	-21.5
	St.106-03	106.5	20.4	6.2	66.7	-23.5
	St.106-10	118.6	19.6	7.3	112.1	-24.7
	St.107-07	150.4	21.2	8.5	131.3	-24.2
	St.209-07	160.7	24.8	8.0	75.9	-24.3
AUG.	St.102-09	151.3	13.0	13.3	756.2	-25.2
	St.103-09	165.3	15.8	14.5	599.1	-25.2
	St.104-04	144.6	13.7	12.4	614.3	-23.6
	St.104-11	162.7	15.0	12.3	1078.9	-24.0
	St.105-07	185.2	12.7	15.8	1328.0	-24.9
	St.105-11	187.6	18.2	12.7	904.5	-24.4
	St.106-05	201.3	17.9	14.2	532.7	-18.8
	St.107-03	205.4	16.8	14.4	773.2	-23.5
	St.107-07	150.3	16.7	10.8	691.5	-23.3
	St.209-07	183.2	17.1	12.6	667.4	-23.0
OCT.	St.102-07	137.0	18.8	8.5	112.7	-21.7
	St.103-05	143.2	19.6	9.3	134.5	-21.8
	St.103-09	121.1	18.8	7.7	150.3	-21.5
	St.104-08	183.9	41.0	5.4	88.2	-21.5
	St.105-03	96.7	20.2	5.8	103.7	-22.3
	St.105-11	93.3	18.8	6.2	125.5	-22.0
	St.106-07	71.8	13.8	6.3	189.0	-21.2
	St.107-03	135.7	24.4	6.8	121.3	-22.0
	St.107-07	74.2	15.0	6.2	188.6	-22.1
	St.209-04	110.1	21.5	6.3	93.1	-23.5

composition-environment correlations of 0.799 on the first axis and 0.616 on the second axis (Table 5). The Monte Carlo permutation test (999 permutations under full model) found that both the first canonical axis and the sum of all canonical axes were significant (F = 25.901, p = 0.001, and F = 3.904, p = 0.001, respectively), which indicated that environmental variables well explained the biochemical compositions of bulk POM.

The RDA triplot (Figure 6) illustrates the relationships among the probabilities for biochemical compositions of POM (biomolecular and AA compositions) and environment variables during this study. In the RDA triplot, the orientations of samples collected from February and April were markedly distinguished along the first ordination axis (Figure 6). Results of the RDA suggest that CHO, HIS, and ΣEAA% were positively correlated

10.3389/fmars.2022.979137

TABLE 4 Depth-weighted average concentrations of each biomolecular compound (CHO, PRT, and LIP) and food materials (FM; the sum of CHO, PRT, and LIP concentrations) and percentages of the biomolecular composition of POM in southwestern East/Japan Sea, 2018.

Month	Station	depth-weighted average concentration (μg L^{-1})				Composition (%)		
		CHO	PRT	LIP	FM	CHO	PRT	LIP
FEB.	St.103-07	130.3	22.7	53.9	206.9	62.7	11.2	26.1
	St.103-11	100.2	40.2	75.1	215.6	46.6	18.7	34.7
	St.105-05	123.6	10.1	57.1	190.8	62.0	7.1	30.9
	St.105-07	172.6	15.7	70.0	258.2	68.4	6.0	25.6
	St.105-11	182.7	13.8	58.4	254.9	69.4	5.5	25.1
	St.107-05	149.5	24.1	73.6	247.3	62.0	8.7	29.3
	St.107-07	111.3	2.7	62.5	176.4	62.8	2.4	34.8
	St.209-05	145.8	10.8	59.6	216.1	68.7	3.5	27.9
	St.209-08	124.6	15.4	71.1	211.1	69.0	4.7	26.3
APR.	St.102-06	72.3	88.6	79.7	240.6	35.2	32.9	31.9
	St.103-04	253.9	95.0	122.8	471.8	54.5	20.7	24.9
	St.103-10	154.2	147.4	155.5	457.1	36.1	28.7	35.1
	St.104-05	120.0	93.9	98.2	312.1	39.1	29.1	31.8
	St.104-09	122.6	90.9	112.3	325.8	37.2	28.3	34.5
	St.105-10	138.5	71.1	83.7	293.4	48.4	22.9	28.7
	St.106-03	119.2	88.7	87.7	295.5	42.4	28.0	29.7
	St.106-10	130.8	66.0	93.2	290.1	44.9	23.2	32.0
	St.107-07	134.9	106.0	107.0	347.9	39.8	29.8	30.4
	St.209-07	152.2	77.7	102.5	332.4	44.6	25.0	30.4
AUG.	St.102-09	73.9	21.6	49.4	144.9	54.5	13.2	32.3
	St.103-09	71.1	16.9	61.6	149.6	50.5	11.6	37.9
	St.104-04	75.1	11.4	44.3	130.8	59.0	8.6	32.4
	St.104-11	77.4	15.8	64.8	158.0	48.6	12.7	38.6
	St.105-07	84.2	16.1	64.4	164.8	52.9	10.9	36.2
	St.105-11	89.5	21.0	61.4	171.8	55.8	10.8	33.4
	St.106-05	84.0	37.2	66.0	187.3	49.0	18.3	32.8
	St.107-03	85.8	28.0	68.5	182.4	49.6	14.6	35.8
	St.107-07	100.8	22.1	61.6	184.6	55.5	11.0	33.5
	St.209-07	96.0	23.9	68.3	188.2	51.3	13.1	35.6
OCT.	St.102-07	77.8	39.3	118.4	235.5	35.6	16.2	48.2
	St.103-05	92.4	36.5	124.7	253.5	39.1	13.4	47.5
	St.103-09	60.0	33.5	117.4	210.8	30.7	15.9	53.4
	St.104-08	117.5	111.5	157.7	386.7	33.0	26.4	40.6
	St.105-03	104.7	34.7	92.0	231.4	46.1	14.5	39.3
	St.105-11	87.3	42.5	116.3	246.1	36.5	17.2	46.3
	St.106-07	75.3	19.9	145.4	240.6	32.2	10.3	57.5
	St.107-03	116.5	52.1	107.1	275.7	44.1	17.3	38.6
	St.107-07	76.8	20.2	102.8	199.8	38.6	10.6	50.8
	St.209-04	88.9	42.8	109.1	240.8	40.8	16.6	42.6

with major inorganic nutrients (SiO_2, PO_4, and NO_2+NO_3) except for NH4 and associated with February. In contrast, PRT, ΣNEAA%, and SER were explained by Dino, Prymnesio, and NH_4 and were largely associated with April (Figure 6). According to the second ordination axis, LIP, LEU, and ALA were positively correlated with Chloro, Temp, and Cyano, and oriented opposite to Prasino and Sal (Figure 6).

Discussion

Characteristics of the bulk POM

Generally, POM is a heterogeneous mixture of various particulate matters including autotrophic and heterotrophic organisms, detrital components, and terrestrial organic matters

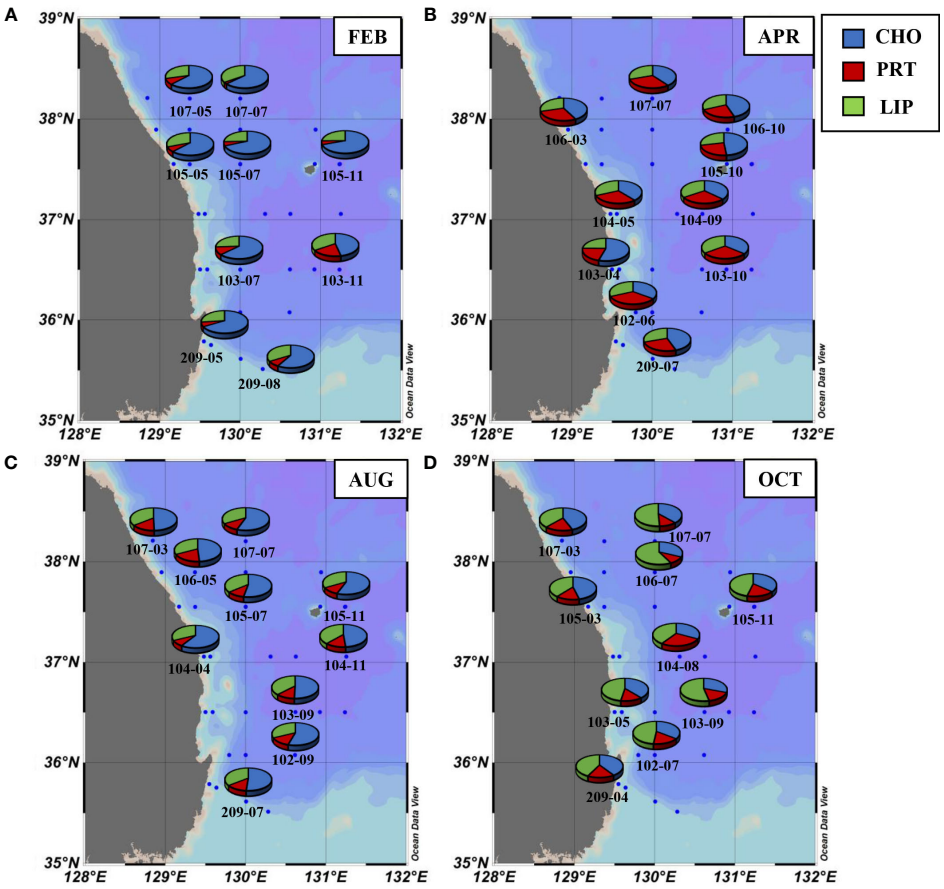

FIGURE 2
Spatial distribution of the biomolecular composition of POM averaged from three different light depths (100, 30, and 1%) in **(A)** February, **(B)** April, **(C)** August, and **(D)** October.

(Harmelin-Vivien et al., 2008). Molar carbon to nitrogen (C/N ratio), POC/Chl-*a* ratio, and stable isotope of organic carbon ($\delta^{13}C$) can be widely used for identifying the source of POM in marine environments (Gearing et al., 1984; Zweifel et al., 1993; Savoye et al., 2003). The range of C/N ratios except August varied from 5.4 to 11.0 (mean ± S.D = 7.7 ± 1.7) in this study (Table 3), which indicates a dominant contribution of marine phytoplankton to POM ranging from 6 to 10 (Meyers, 1994; Montagnes et al., 1994; Tyson, 1995). However, the high C/N ratios of POM (10.8 – 15.8; an average of 13.3) were observed in August compared with those in other seasons (Table 3). Moreover, the low chl-*a* concentrations (0.1 – 0.4 μg L^{-1}) and high POC/Chl-*a* ratios (532.7 – 1328.0) obtained in August could be related to high contributions of non-autotrophic materials (Tables 2 and 3) (Frigstad et al., 2011). Normally, POC/Chl-*a* ratios lower than 200 indicate that POM is mainly composed of afresh-produced phytoplankton and/or autotrophic organisms, whereas the ratios higher than 200 are indicative of detrital and degraded materials or heterotrophic dominated organic matter (Savoye et al., 2003). Therefore, the POM in August could be a mixture of non-autotrophic materials and degraded and phytodetrital organic matter. Compared to the C/N ratio ranging from -23 to -19 ‰ (Fry and Sherr, 1989; Middelburg and Herman, 2007; Harmelin-Vivien et al., 2008), spatial and seasonal variations in $\delta^{13}C$ of the surface bulk POM were not observed throughout this study, although the ranges were wide varying from -26.3 to -18.8 ‰ (mean ± S.D = -23.3 ± 1.5 ‰) (Table 3). Although the $\delta^{13}C$ values in our POM samples were found relatively lower than the carbon isotopic range of typical marine phytoplankton, $\delta^{13}C$ values in company with other indicators (C/N and POC/Chl-*a* ratios) suggest that the POM in our samples was sourced mainly from phytoplankton and phytoplankton-derived phytodetritus.

Seasonal variation in the biomolecular composition of POM

In this study, CHO were most predominant among three biomolecules accounting for 48.6% of the bulk POM followed by

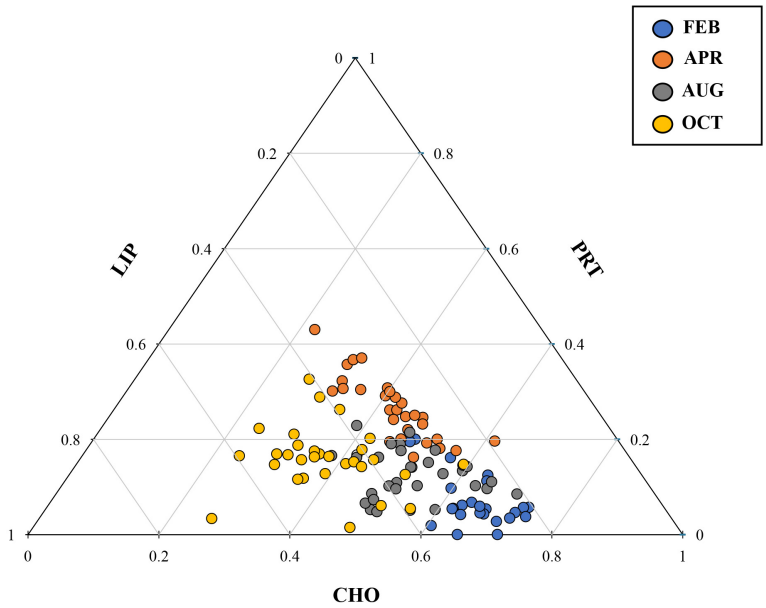

FIGURE 3
Ternary diagram illustrating the relative proportions of CHO, PRT, and LIP in POM during this study.

LIP (35.5%) and PRT (15.9%) (Table 4), which is consistent with the CHO-rich POM previously observed in the southwestern East/Japan Sea (Jo et al., 2017; Jo et al., 2018). However, a considerable seasonal difference in the biomolecular composition of POM was observed from February to October during this study (Figures 2 and 3). This seasonal variation in the biomolecular composition could be explained by the seasonal cycle of phytoplankton biomass and bloom. Typically, the East/Japan Sea has a bimodal pattern of spring and autumn blooms (Vinogradov et al., 1996; Kim et al., 2000; Choi et al., 2016).

In February, we found substantial proportions of CHO (> ca. 50%) and considerably lower PRT composition (7.5 ± 5.0%) of POM (Table 4 and Figure 2A). During winter, phytoplankton encounter low temperature and light intensity along with deep turbulent vertical mixing within the euphotic zone (Townsend et al., 1992). When phytoplankton are exposed to these conditions, they have mechanisms to adapt to the winter season by suppressing metabolic activity (Antia, 1976; Peters, 1996; Furusato et al., 2004). In this study, the mixed layer depths were shallower than their euphotic depths at some stations (st. 103-07, 105-07, 105-11, and 107-07) (Table 1), indicating weak mixing conditions during late winter. However, lower chl-*a* concentrations were observed in February (Table 2), despite high concentrations of inorganic nutrients (phosphate, nitrate + nitrite, and silicate) within the euphotic zone (Table 1). The CHO-rich and PRT-low POM in February could be explained by the reduction in physiological activity.

The mean PRT composition of POM in April (mean ± S.D. = 26.9 ± 3.8%) was ca. 4 folds as high as that in February (mean ± S.D. = 7.5 ± 5.0%) (Table 4). The higher concentrations of total chl-*a* and FM in April (Tables 2 and 4) could have been related to the spring bloom of phytoplankton (Yoo and Kim, 2004; Choi et al., 2016). The concentrations of phosphate, and nitrate + nitrite throughout the euphotic zone in April were lower than those in February (Table 1) and showed remarkable negative relationships with total chl-*a* concentration (DIP vs. Chl-*a*: $r = -0.739$, $p < 0.01$, $n = 30$; NO_2+NO_3 vs. Chl-*a*: $r = -0.709$, $p < 0.01$, $n = 30$). This suggests that phosphate and nitrate + nitrite concentrations were consumed by the phytoplankton growth during the spring bloom. In contrast with those in February, relatively higher PRT and lower CHO compositions prevailed during the spring bloom was associated with high phytoplankton biomass, and active growth conditions (Morris, 1981; Ríos et al., 1998; Jo et al., 2021).

An increase in CHO proportion and lower PRT contribution in the bulk POM reappeared in August (Table 4 and Figure 2C), which is most likely connected with phytodetrital and degraded materials in August as mentioned above. During summer, enhanced degradation of most bioavailable materials especially more N-rich compounds (e.g. PRT) than C-rich (e.g. CHO and LIP) is progressed by elevated temperatures and solar irradiation (Álvarez-Salgado et al., 2006; Lønborg et al., 2017). The increasing temperature could accelerate PRT decomposition because of the activity of PRT degrading enzymes along with growth in the bacterial community (Piontek et al., 2009; Ye et al., 2017) and also lead to reducing PRT synthesis of phytoplankton (Konopka and Brock, 1978; Thompson et al., 1992; Lee et al., 2017a). Especially in the summer of 2018, the longest heatwave period and highest air temperature were reported in the East/Japan Sea (Wie et al., 2021). Consistently, very high sea surface

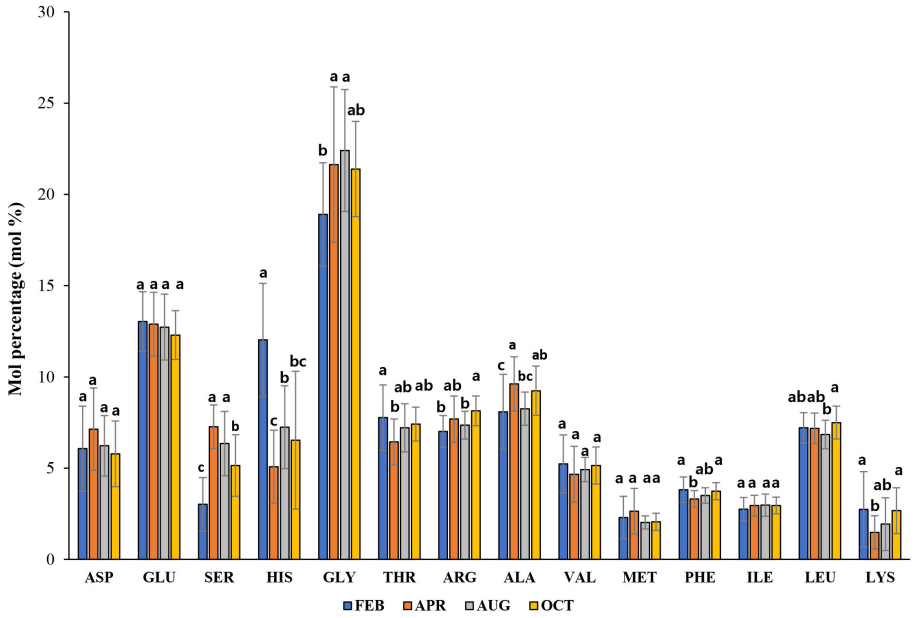

FIGURE 4
Average mol percentages of individual PAA in the bulk POM during four sampling months. Different letters indicate significant differences by Scheffe's method ($p < 0.05$).

temperatures (up to 29.15°C; Table 1) were observed in August during this study.

The relatively predominant LIP (mean ± S.D. = 46.5 ± 6.3%) observed during October in this study is similar to those in the East/Japan Sea previously reported by Kang et al. (2017) and Jo et al. (2018) (Table 4 and Figure 2D). Therefore, the higher incorporation of carbon to LIP during the fall season in the East/Japan Sea could be a seasonal characteristic pattern of the photosynthetic carbon allocations of phytoplankton. Under nitrogen-depleted or/and other non-optimized conditions, microalgae can accumulate CHO rather than LIP, whereas can promote the accumulation of reserve LIP in place of CHO as these stresses persist (Hu, 2013; reference therein). In other words, they can store secondary carbon and energy reserve in the form of triacylglycerol for the long-term survival of microalgae under stress-inducing conditions (Hu, 2013). Considering the possibility of continuous nutrient stress, the relatively predominant LIP during October in this study could result from long-lasting nutrient stress conditions induced by thermal stratification from summer. Indeed, high levels of inorganic nutrient concentrations were found only at the 1% light depths (Table 1).

Seasonal variations in the AA composition of POM and AA indices

PAA concentrations in this study varied from 0.07 to 1.71 μM in accordance with seasons, stations, and sampling depths (Supplementary Table 1). They were correlated with total chl-*a* concentration, which is consistent with previous studies conducted in temperate oceans (Chen et al., 2004; Chen et al., 2021; Kuznetsova et al., 2004; Unger et al., 2005; Ji et al., 2019; Liu and Xue, 2020; Alyuruk and Kontas, 2021). Furthermore, this result along with a positive correlation between PAA and total PRT concentrations suggests that the production of PAA was mainly derived from the PRT of phytoplankton in this study (Jo et al., 2021).

Dominant AA constituents in PAA measured during this study were GLY, GLU, and ALA in this order (Figure 4). This is in agreement with the previous findings that dominant AA forms are similar in various ocean areas (Tsukasaki and Tanoue, 2010; Wu et al., 2016; Zhang et al., 2016; Alyuruk and Kontas, 2021; Jo et al., 2021). The predominance of GLY composition (> ca. 20 mol%) has been reported in POM (Liebezeit and Bölter, 1986; Shields et al., 2019; Jo et al., 2021) as well as DOM and sediments in marine environments (Dauwe and Middelburg, 1998; Duan and Bianchi, 2007; Wu et al., 2016; Zhang et al., 2016). The high proportion of GLY is generally attributed to the degradation product of the other AAs and structural material due to increased microbial activity (Lee and Cronin, 1984; Dauwe and Middelburg, 1998). As microbial degradation proceeds, GLY enriched in the cell wall material is protected against degradation, resulting in the accumulation of GLY in decomposing POM (Lee and Cronin, 1984; Dauwe and Middelburg, 1998). In contrast, GLU is an important component

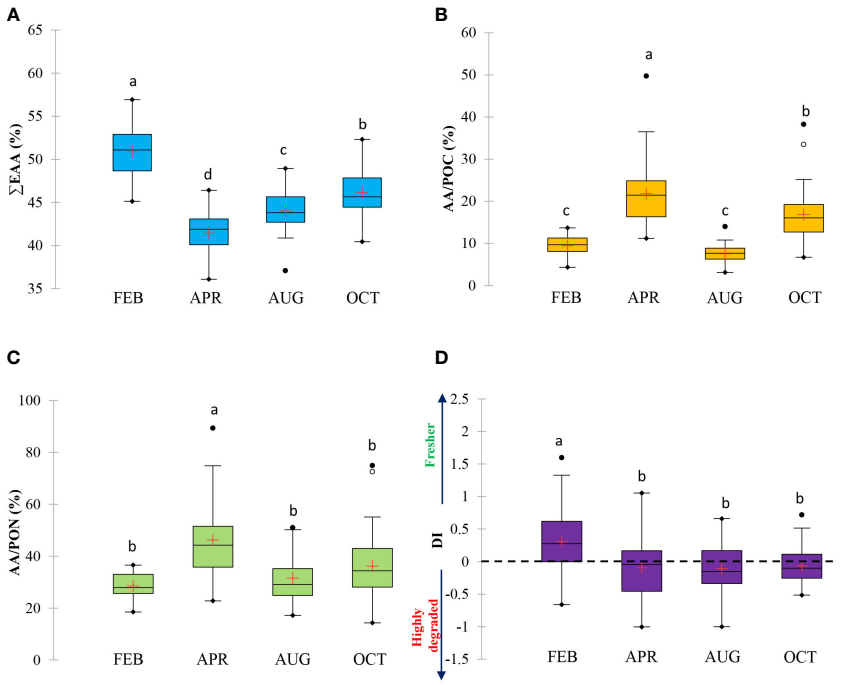

FIGURE 5
Boxplots of **(A)** total EAA composition (∑EAA%), **(B)** carbon and **(C)** nitrogen normalized yields of PAA (AA-POC% and AA-PON%), and **(D)** degradation index (DI). Different letters indicate significant differences by Scheffe's method ($p < 0.05$).

of intracellular PRT and indicative of fresh POM since its abundance is higher in the cytoplasm and tends to be decreased during degradation (Lee and Cronin, 1984; Dauwe and Middelburg, 1998; Sheridan et al., 2002). Therefore, the overall AAs characteristics of our POM samples during this study were structural AAs (such as GLY and ALA; Hecky et al., 1973) and GLU common in the fresh materials (Lee and Cronin, 1984; Dauwe and Middelburg, 1998), indicating that POM was the mixtures of decomposing material and fresher POM.

In various oceans, typically the AA-POC% and AA-PON% contribute ca. 30% of POC and ca. 50% of PON, respectively, although they are variable (Tsukasaki and Tanoue, 2010). On the average, AA accounted for 14.3 ± 8.1% (3.1 – 49.7%) of total POC and 35.8 ± 13.4% (14.3 – 89.3%) of total PON throughout this study (Supplementary Table 1). These values are somewhat lower than typical levels in the suspended POM (Supplementary Table 2). The contribution of AA to the total POC reflects the freshness of POM and the bloom phase of phytoplankton (Davis et al., 2009; Shields et al., 2019). In general, the AA-POC% decreases with enhanced degradation, since AA-containing compounds (e.g., PRT) have a higher susceptibility to microbial degradation than other compounds (Davis et al., 2009; Shields et al., 2019). Furthermore, POM derived from phytoplankton in the mid-exponential growth phase has higher AA-POC% values, while lower AA-POC% is found during stationary and decomposition phases of phytoplankton (Shields et al., 2019). The values of AA-POC% in April (22.1 ± 8.1%) are significantly higher than those in other seasons (Figure 5B; one-way ANOVA, $p < 0.05$), indicating that POM contained more fresh organic materials during the spring bloom period (Lehmann et al., 2020). In contrast, we observed significantly lower AA-POC yields in February and August (Figure 5B; 9.5 ± 2.3% and 7.5 ± 2.3%; one-way ANOVA, $p < 0.05$), indicating that POM during these periods contained high quantities of other C-rich materials such as degraded detritus or transparent exopolymer particle (TEP) related with particulate CHO (Shields et al., 2019). In consistency with AA-POC%, AA-PON% could also be indicated for diagenesis of POM and fresh phytoplankton (Duan and Bianchi, 2007; Zhu et al., 2016). The higher values of AA-PON% also were found in April with a spring phytoplankton bloom (Figure 5C). However, no significant difference in AA-PON% was found among other seasons (Figure 5C; one-way ANOVA, $p > 0.05$). Therefore, AA-POC% could be a more sensitive indicator for the freshness of POM and the bloom phase of phytoplankton than AA-PON%.

Like the AA-POC% and AA-PON%, the DI scores for the exponential growth phase including fresh POM have more positive values while those in the stationary or degradation phase have more negative values (Duan and Bianchi, 2007; Zhu et al., 2016). However, we found higher values of DI in

10.3389/fmars.2022.979137

TABLE 5 Ordination results of the RDA during this study.

RDA Axes	1	2	3	4	Total variance
Eigenvalues	0.204	0.047	0.034	0.015	1
Biochemical compositions -environment correlations	0.799	0.616	0.538	0.471	
Cumulative percentage variance of biochemical compositions data	20.4	25.1	28.5	30	
Cumulative percentage variance of biochemical compositions-environment relationship	61	75.2	85.3	89.7	
Sum of all eigenvalues					1
Sum of all canonical eigenvalues					0.334

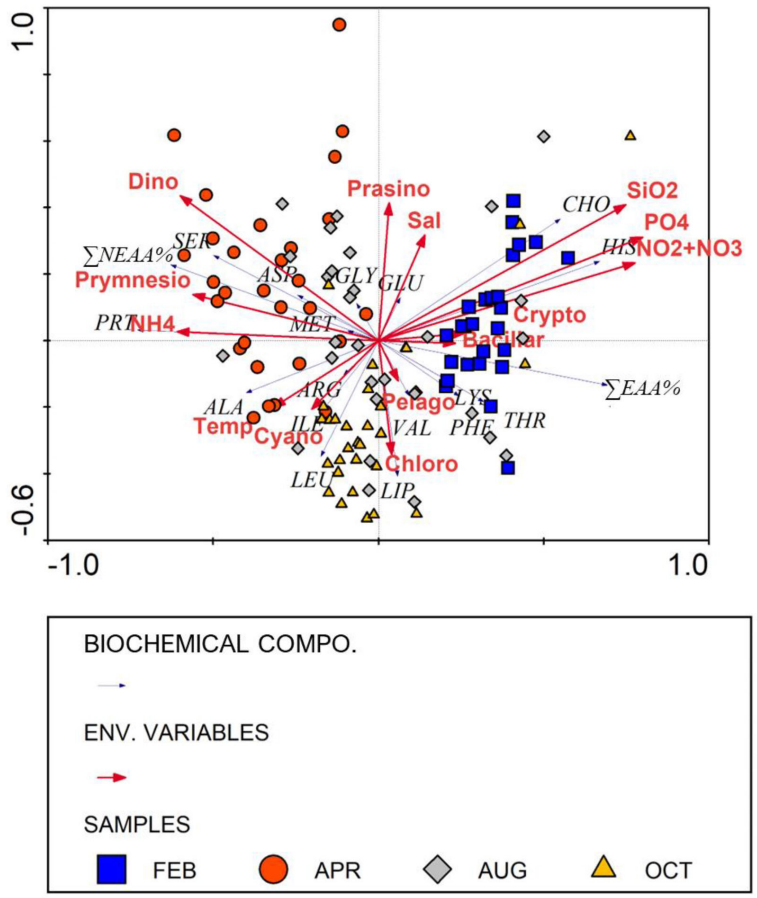

FIGURE 6
Results of the redundancy analysis (RDA) for biochemical compositions (biomolecular and AA compositions) of POM in relation to environmental variables sampled in the southwestern East/Japan Sea from February to October 2018. Each abbreviation represents as Aspartic acid (ASP), Glutamic acid (GLU), Serine (SER), Histidine (HIS), Glycine (GLY), Threonine (THR), Arginine (ARG), Alanine (ALA), Valine (VAL), Methionine (MET), Phenylalanine (PHE), Isoleucine (ILE), Leucine (LEU), Lysine (LYS), non/essential amino acid composition (∑NEAA%, ∑EAA%), biomolecular composition (CHO, PRT, and LIP), relative contributions of Prasinophytes (Prasino), Dinophytes (Dino), Cryptophytes (Crypto), Prymnesiophytes (Prymnesio), Pelagophytes (Pelago), Chlrophytes (Chloro), Cyanophytes (Cyano), and Bacillatiophytes (Bacillar), temperature (Temp), salinity (Sal), phosphate (PO_4), nitrate + nitrite (NO_2+NO_3), ammonium (NH_4), and silicate (SiO_2).

February (Figure 5D; -0.72 – 2.17; one-way ANOVA, $p< 0.05$), which does not correspond to the degradation state based on the AA-POC% and AA-PON%. AA-POC% and AA-PON% have been used as the most sensitive indicators of initial degradation stages, whereas the DI can be more suitable for intermediate timescales (Dauwe et al., 1999; Wu et al., 2007; Shields et al., 2019). Furthermore, DI scores can be influenced by sources of POM, and therefore, they could not provide a clear distinction

between the influences of source and degradation (Ingalls et al., 2003; Zhang et al., 2016). In calculating a DI score, enriched GLY in POM has more negative loading because GLY is preferentially preserved relative to other AAs during degradation (Lee and Cronin, 1984; Ingalls et al., 2003). On the other hand, a high proportion of GLY was observed in diatom-dominated phytoplankton communities (2006; Ingalls et al., 2003). Thus, POM including a large number of diatom cells can have lower DI values (Keil et al., 2000; Ingalls et al., 2003). However, no relationship between GLY and diatoms was found in this study ($p > 0.05$). Although diatoms (33.6 ± 22.5%) were the dominant algal group throughout this study period, spatial and temporal variations in phytoplankton community compositions appeared complicatedly (Table 2). Therefore, the DI value inconsistent with AA-POC% and AA-PON% could be caused by a combination of source effect and degradation of POM in this study (Ingalls et al., 2003; Zhang et al., 2016). Taking our results into account, a combined evaluation of degradation indicators is necessary to avoid faulty interpretation, especially for seasonal snapshots of the AA data sets.

Drivers of PRT quality associated with EAA under different sampling seasons

The PRT quality can be evaluated by the ΣEAA% which has a direct effect on nutritional quality for higher trophic levels (Ju et al., 2008). Field and laboratory studies have shown that ΣEAA % in microalgae and cyanobacteria communities are rather stable within a narrow range (from 41 to 55%) (Kolmakova and Kolmakov, 2019 and the reference therein). However, ΣEAA % during this study had a relatively wider range (36.1 – 56.9%; Supplementary Table 1) and a clear season difference (Figure 5A). Furthermore, the most striking feature of ΣEAA% throughout this whole study was a particularly strong negative correlation with PRT composition (Figure 6; Pearson's correlation: $r = -0.615$, $n = 115$, $p < 0.01$). Such a relationship can be largely attributed to nutrient availability (especially nitrogen) because the biosynthesis of EAAs is far more influenced by nutrient availability than NEAAs because EAAs are synthesized from the conversion of NEAAs as a precursor and therefore require additional processes and enzyme reactions (Grosse et al., 2019; Grosse et al., 2020). Since the reductions of these several additional steps and enzyme production are beneficial for phytoplankton under N-limited conditions, the conversion of NEAAs to EAAs could substantially be decreased (Grosse et al., 2017; Grosse et al., 2019). In the present study, we used< 1 μM absolute dissolved inorganic nitrogen (DIN: nitrite + nitrate + ammonium) concentration and an N/P ratio of< 10 to assess nitrogen limitation (Justić et al., 1995; Jo et al., 2018). Although DIN concentration and N/P ratio below threshold values that determine nitrogen limitation were observed in the whole upper layer in August (Table 1), a pervasive nitrogen limitation could not be inferred from those observations during other three seasons. However, ambient nutrient concentrations and stoichiometric ratios cannot be always the best predictors for nutrient limitation because their interpretations are complicated by excessive uptake of nutrients in deficient cells (Healey, 1979; Lean and Pick, 1981) and different nutrient requirements of diverse algal groups (Ho et al., 2003). Therefore, nitrogen availability for phytoplankton could be supported by the biochemical compositions as indicators of nutrient status (Morris et al., 1974; Dortch and Whitledge, 1992). RDA results in this study demonstrated obvious seasonal distinctions in the biochemical compositions of POM between February and April (Figure 6), which may be due to the consequences of nutrient availability. We found that EAAs (particularly HIS) were associated with higher nutrient concentrations (except for ammonium) in this study (Figure 6). In winter, a strong water mixing induced by the Asian monsoon and a low phytoplankton nutrient uptake caused by weak solar radiation and short photoperiod induce accumulated inorganic nutrients in the whole euphotic zone (Lim et al., 2012; Baek et al., 2020). Consequently, the increased nutrient loading could have enhanced the biosynthesis of EAAs more than NEAAs in phytoplankton communities, although the lower PRT composition of POM indicated a physiologically inactive status of phytoplankton. In comparison, higher PRT compositions in April were associated with the active growth phase of phytoplankton during the spring bloom period, while relatively lower availability of ambient nutrients in response to the high nutrient consumption of increased phytoplankton biomass could have caused phytoplankton to convert insufficiently EAAs from NEAAs, which subsequently lowered ΣEAA%. Furthermore, our RDA result revealed significant positive relationships between flagellates (including dinoflagellates and prymnesiophytes) and ΣNEAA% in this study (Figure 6). Under nitrogen-limited conditions, flagellate-dominated communities show an apparent qualitative shift toward NEAAs compared to diatom-dominated communities (Grosse et al., 2019). Therefore, the relative qualitative changes in contributions of EAAs and NEAAs during our study could have been greatly influenced by the ambient nutrient availability or/and changes in phytoplankton community composition (Grosse et al., 2020).

Summary and conclusions

This study found seasonal differences in the relative dominance of biochemical (biomolecular and AA) compositions of bulk POM associated with the bloom/growth phase and seasonal physiological condition of phytoplankton communities in the East/Japan Sea. Although CHO were predominant overall, PRT and LIP compositions increased during the spring and autumn bloom periods. Moreover, a

negative correlation between PRT and ΣEAA% was also found in this study, indicating that PRT quality and partition of EAAs and NEAAs could be influenced by seasonal nutrient availability as well as phytoplankton community composition. These changes in the biochemical (biomolecular and AA) compositions of bulk POM mainly derived phytoplankton could have significant ecological implications for bacterial degradation and recycling (Ingalls et al., 2006; Sabadel et al., 2019; Lehmann et al., 2020) and higher trophic levels as potential prey (Guisande et al., 2000; Vargas et al., 2006; Jo et al., 2021). Especially, the PRT quality with respect to AA composition of POM deserves a greater attention because adequate availability of EAAs in potential prey is crucial for the optimal growth and reproduction of zooplankton (Kolmakova and Kolmakov, 2019). Although we cannot directly assess food quality for herbivores by correlation and similarity analyses between biochemical compositions of POM and zooplankton (Jo et al., 2017; Jo et al., 2021), we identified seasonal dynamics and potential drivers of biochemical compositions in phytoplankton-derived POM which could be ecologically associated with zooplankton. This work lays the foundation for evaluating *in situ* dynamics of nutritional quality for herbivores in the southwestern East/Japan Sea.

Under current climate change, the East/Japan Sea has experienced many changes in physical and biogeochemical properties, and subsequently nutrient availability, primary production, and phytoplankton communities (size structure and species composition) (Kim et al., 2001; Chiba et al., 2012; Lee et al., 2017b; Kang et al., 2020). These environmental changes could have impacts on both the quantity and quality of POM in the East/Japan Sea. Further elucidation of the spatial and seasonal variations in biochemical (biomolecular and amino acid) compositions of POM and validation of various relationships with environmental parameters are required to understand changes in nutritional quality as prey and subsequent effects on higher trophic level organisms under ongoing climate changes in the East/Japan Sea. This study could help future studies to understand the climate-induced changes on the quantity and quality of POM in diverse marine ecosystems over broader temporal-spatial scales.

Data availability statement

The original contributions presented in the study are included in the article/Supplementary Material. Further inquiries can be directed to the corresponding author.

Author contributions

NJ, S-HY, and SL contributed conceptualization and design of the study. Samples analysis and data collections were performed by NJ, HTJ, H-KJ, YK, SP, JSK, KK, and JJK. Data curation and validation were performed by NJ, H-KJ, YK, SP, JSK, and KK. S-HY and HTJ provided scientific advice on data interpretation. NJ wrote the first draft of the manuscript. SL reviewed and editing previous versions of the manuscript. All authors contributed to manuscript writing, revision, read and approved the submitted version. All authors agreed with the submission of the manuscript.

Funding

This research was supported by the "Development of assessment technology on the structure variations in marine ecosystem (R2022073)" funded by the National Institute of Fisheries Science (NIFS), Korea, and the National Research Foundation of Korea Grant funded by the Korean Government (NRF-2019R1A2C100351).

Conflict of interest

The authors declare that the research was conducted in the absence of any commercial or financial relationships that could be construed as a potential conflict of interest.

Publisher's note

Supplementary material

The Supplementary Material for this article can be found online at: https://www.frontiersin.org/articles/10.3389/fmars.2022.979137/full#supplementary-material

References

Álvarez-Salgado, X. A., Nieto-Cid, M., Gago, J., Brea, S., Castro, C. G., Doval, M. D., et al. (2006). Stoichiometry of the degradation of dissolved and particulate biogenic organic matter in the NW Iberian upwelling. *J. Geophys. Res. Ocean.* 111, C07017. doi: 10.1029/2004JC002473

Alyuruk, H., and Kontas, A. (2021). Dissolved free, total and particulate enantiomeric amino acid levels in eutrophic and oligotrophic parts of a semi-enclosed bay (İzmir, Aegean Sea). *Reg. Stud. Mar. Sci.* 44, 101750. doi: 10.1016/j.rsma.2021.101750

Andersson, A., Tamminen, T., Lehtinen, S., Jürgens, K., Labrenz, M., and Viitasalo, M. (2017). "The pelagic food web," in *Biological oceanography of the Baltic Sea* (Dordrecht: Springer), 281–332.

Antia, N. J. (1976). Effects of temperature on the darkness survival of marine microplanktonic algae. *Microb. Ecol.* 3 (1), 41-54. doi: 10.1007/BF02011452

Baek, S. H., Lee, M., Park, B. S., and Lim, Y. K. (2020). Variation in phytoplankton community due to an autumn typhoon and winter water turbulence in southern korean coastal waters. *Sustain.* 12 (7), 2781. doi: 10.3390/su12072781

Bartolomeo, M. P., and Maisano, F. (2006). Validation of a reversed-phase HPLC method for quantitative amino acid analysis. *J. Biomol. Tech.* 17, 131–137.

Bhavya, P. S., Kim, B. K., Jo, N., Kim, K., Kang, J. J., Lee, J. H., et al. (2019). A review on the macromolecular compositions of phytoplankton and the implications for aquatic biogeochemistry. *Ocean. Sci. J.* 54 (1), 1–14. doi: 10.1007/s12601-018-0061-8

Bligh, E. G., and Dyer, W. J. (1959). A rapid method of total lipid extraction and purification. *Can. J. Biochem. Physiol* 37, 911-917. doi: 10.1139/o59-099

Chen, J., Li, Y., Yin, K., and Jin, H. (2004). Amino acids in the pearl river estuary and adjacent waters: Origins, transformation and degradation. *Cont. Shelf Res.* 24 (16), 1877-1894. doi: 10.1016/j.csr.2004.06.013

Chen, Y., Wang, P., Shi, D., Ji, C. X., Chen, R., Gao, X. C., et al. (2021). Distribution and bioavailability of dissolved and particulate organic matter in different water masses of the southern yellow Sea and East China Sea. *J. Mar. Syst.* 222, 103596. doi: 10.1016/j.jmarsys.2021.103596

Chiba, S., Batten, S., Sasaoka, K., Sasai, Y., and Sugisaki, H. (2012). Influence of the pacific decadal oscillation on phytoplankton phenology and community structure in the western north pacific. *Geophys. Res. Lett.* 39, L15603. doi: 10.1029/2012GL052912

Choi, J. K., Noh, J. H., Orlova, T., Park, M.-O., Lee, S. H., Park, Y.-J., et al. (2016). ""Phytoplankton and primary production,"," in *Oceanography of the East Sea (Japan Sea)*. Eds. K.-I. Chang, C.-I. Zhang, C. Park, D.-J. Kang, S.-J. Ju, S.-H. Lee, et al (Cham: Springer International Publishing), 217–245. doi: 10.1007/978-3-319-22720-7_10

Crosbie, N. D., and Furnas, M. J. (2001). Abundance, distribution and flow-cytometric characterization of picophytoprokaryote populations in central (17°S) and southern (20°S) shelf waters of the great barrier reef. *J. Plankton Res.* 23, 809-828. doi: 10.1093/plankt/23.8.809

Danovaro, R., Dell'Anno, A., Pusceddu, A., Marrale, D., Della Croce, N., Fabiano, M., et al. (2000). Biochemical composition of pico-, nano- and micro-particulate organic matter and bacterioplankton biomass in the oligotrophic Cretan Sea (NE Mediterranean). *Prog. Oceanogr.* 46 (2-4), 279-310. doi: 10.1016/S0079-6611(00)00023-9

Dauwe, B., and Middelburg, J. J. (1998). Amino acids and hexosamines as indicators of organic matter degradation state in north Sea sediments. *Limnol. Oceanogr.* 43, 782–798. doi: 10.4319/lo.1998.43.5.0782

Dauwe, B., Middelburg, J. J., Herman, P. M. J., and Heip, C. H. R. (1999). Linking diagenetic alteration of amino acids and bulk organic matter reactivity. *Limnol. Oceanogr.* 44, 1809–1814. doi: 10.4319/lo.1999.44.7.1809

Davis, J., Kaiser, K., and Benner, R. (2009). Amino acid and amino sugar yields and compositions as indicators of dissolved organic matter diagenesis. *Org. Geochem.* 40, 343–352. doi: 10.1016/j.orggeochem.2008.12.003

Dortch, Q., and Whitledge, T. E. (1992). Does nitrogen or silicon limit phytoplankton production in the Mississippi river plume and nearby regions? *Cont. Shelf Res.* 12, (11), 1293-1309. doi: 10.1016/0278-4343(92)90065-R

Duan, S., and Bianchi, T. S. (2007). Particulate and dissolved amino acids in the lower Mississippi and pearl rivers (USA). *Mar. Chem.* 107, 214–229. doi: 10.1016/j.marchem.2007.07.003

Dubois, M., Gilles, K. A., Hamilton, J. K., Rebers, P. A., and Smith, F. (1956). Colorimetric method for determination of sugars and related substances. *Anal. Chem* 28 (3), 350-356. doi: 10.1021/ac60111a017

Dzierzbicka-Głowacka, L., Kuliński, K., Maciejewska, A., Jakacki, J., and Pempkowiak, J. (2010). Particulate organic carbon in the southern baltic sea: Numerical simulations and experimental data. *Oceanologia* 52 (4), 621-648. doi: 10.5697/oc.52-4.621

Fernández-Reiriz, M. J., Perez-Camacho, A., Ferreiro, M. J., Blanco, J., Planas, M., Campos, M. J., et al. (1989). Biomass production and variation in the biochemical profile (total protein, carbohydrates, RNA, lipids and fatty acids) of seven species of marine microalgae. *Aquaculture* 83 (1-2), 17-37. doi: 10.1016/0044-8486(89)90057-4

Frigstad, H., Andersen, T., Hessen, D. O., Naustvoll, L. J., Johnsen, T. M., and Bellerby, R. G. J. (2011). Seasonal variation in marine C:N:P stoichiometry: Can the composition of seston explain stable redfield ratios? *Biogeosciences* 8, 2917–2933. doi: 10.5194/bg-8-2917-2011

Fry, B., and Sherr, E. B. (1989). doi: 10.1007/978-1-4612-3498-2_12

Furusato, E., Asaeda, T., and Manatunge, J. (2004). Tolerance for prolonged darkness of three phytoplankton species, microcystis aeruginosa (Cyanophyceae), scenedesmus quadricauda (Chlorophyceae), and melosira ambigua (Bacillariophyceae). *Hydrobiologia* 527 (1), 153-162. doi: 10.1023/B:HYDR.0000043198.08168.d3

Gearing, J. N., Gearing, P. J., Rudnick, D. T., Requejo, A. G., and Hutchins, M. J. (1984). Isotopic variability of organic carbon in a phytoplankton-based, temperate estuary. *Geochim. Cosmochim. Acta* 48, 1089–1098. doi: 10.1016/0016-7037(84)90199-6

Geider, R. J., and La Roche, J. (2002). Redfield revisited: Variability of C:N:P in marine microalgae and its biochemical basis. *Eur. J. Phycol.* 37 (1), 1-17. doi: 10.1017/S0967026201003456

Grosse, J., Brussaard, C. P. D., and Boschker, H. T. S. (2019). Nutrient limitation driven dynamics of amino acids and fatty acids in coastal phytoplankton. *Limnol. Oceanogr.* 64, 302–316. doi: 10.1002/lno.11040

Grosse, J., Burson, A., Stomp, M., Huisman, J., and Boschker, H. T. S. (2017). From ecological stoichiometry to biochemical composition: Variation in n and p supply alters key biosynthetic rates in marine phytoplankton. *Front. Microbiol.* 8. doi: 10.3389/fmicb.2017.01299

Grosse, J., Endres, S., and Engel, A. (2020). Ocean acidification modifies biomolecule composition in organic matter through complex interactions. *Sci. Rep.* 10, 1–14. doi: 10.1038/s41598-020-77645-3

Guisande, C., Riveiro, I., and Maneiro, I. (2000). Comparisons among the amino acid composition of females, eggs and food to determine the relative importance of food quantity and food quality to copepod reproduction. *Mar. Ecol. Prog. Ser.* 202, 135–142. doi: 10.3354/meps202135

Han, I.-S., and Lee, J.-S. (2020). Change the annual amplitude of Sea surface temperature due to climate change in a recent decade around the Korean peninsula. *J. Korean Soc Mar. Environ. Saf.* 26, 233–241. doi: 10.7837/kosomes.2020.26.3.233

Harmelin-Vivien, M., Loizeau, V., Mellon, C., Beker, B., Arlhac, D., Bodiguel, X., et al. (2008). Comparison of c and n stable isotope ratios between surface particulate organic matter and microphytoplankton in the gulf of lions (NW Mediterranean). *Cont. Shelf Res* 28 (15), 1911-1919. doi: 10.1016/j.csr.2008.03.002

Healey, F. P. (1979). Short-term responses of nutrient-deficient algae to nutrient addition. *J. Phycol.* 15 (3), 289-299. doi: 10.1111/j.0022-3646.1979.00289.x

Hecky, R. E., Mopper, K., Kilham, P., and Degens, E. T. (1973). The amino acid and sugar composition of diatom cell-walls. *Mar. Biol.* 19, 323–331. doi: 10.1007/BF00348902

Henderson, J. W., Ricker, R. D., Bidlingmeyer, B. A., and Woodward, C. (2000). Rapid , accurate , sensitive , and reproducible HPLC analysis of amino acids. *Amino acid analysis using Zorbax Eclipse-AAA columns and the Agilent* 1100 (1100), 1–10.

Ho, T. Y., Quigg, A., Finkel, Z. V., Milligan, A. J., Wyman, K., Falkowski, P. G., et al. (2003). The elemental composition of some marine phytoplankton. *J. Phycol.* 39 (6), 1145-1159. doi: 10.1111/j.0022-3646.2003.03-090.x

Hu, Q. (2013). "Environmental effects on cell composition," in *Handbook of microalgal culture: Applied phycology and biotechnology, 2nd ed.* (Oxford: Wiley-Blackwell,). pp. 114-122'. doi: 10.1002/9781118567166.ch7

Ingalls, A. E., Lee, C., Wakeham, S. G., and Hedges, J. I. (2003). The role of biominerals in the sinking flux and preservation of amino acids in the southern ocean along 170°W. *Deep. Res. Part II Top. Stud. Oceanogr.* 50, 713–738. doi: 10.1016/S0967-0645(02)00592-1

Ingalls, A. E., Liu, Z., and Lee, C. (2006). Seasonal trends in the pigment and amino acid compositions of sinking particles in biogenic CaCO3 and SiO2 dominated regions of the pacific sector of the southern ocean along 170°W. *Deep. Res. Part I Oceanogr. Res. Pap.* 53, 836–859. doi: 10.1016/j.dsr.2006.01.004

Ji, C. X., Yang, G. P., Chen, Y., and Zhang, P. Y. (2019). Distribution, degradation and bioavailability of dissolved organic matter in the East China Sea. *Biogeochemistry* 142 (2), 189-207. doi: 10.1007/s10533-018-0529-8

Jo, N., Kang, J. J., Park, W. G., Lee, B. R., Lee, J. H., Kim, Y., et al. (2018). Carbohydrate-dominant phytoplankton and protein-high zooplankton in the northern part of the southwestern East/Japan Sea in 2015. *J. Coast. Res.* 85, 371–375. doi: 10.2112/SI85-075.1

Jo, N., Kang, J. J., Park, W. G., Lee, B. R., Yun, M. S. , Lee, J. H., et al. (2017). Seasonal variation in the biochemical compositions of phytoplankton and zooplankton communities in the southwestern East/Japan Sea. *Deep. Res. Part II Top. Stud. Oceanogr.* 143, 82–90. doi: 10.1016/j.dsr2.2016.12.001

Jo, N., La, H. S., Kim, J. H., Kim, K., Kim, B. K., Kim, M. J., et al. (2021). Different biochemical compositions of particulate organic matter driven by major phytoplankton communities in the northwestern Ross Sea. *Front. Microbiol.* 12. doi: 10.3389/fmicb.2021.623600

Ju, Z. Y., Forster, I., Conquest, L., Dominy, W., Kuo, W. C., and David Horgen, F. (2008). Determination of microbial community structures of shrimp floc cultures by biomarkers and analysis of floc amino acid profiles. *Aquac. Res.* 39, 118–133. doi: 10.1111/j.1365-2109.2007.01856.x

Justić, D., Rabalais, N. N., Turner, R. E., and Dortch, Q. (1995). Changes in nutrient structure of river-dominated coastal waters: Stoichiometric nutrient balance and its consequences. *Estuar. Coast. Shelf Sci.* 40, 339-356. doi: 10.1016/S0272-7714(05)80014-9

Kang, J. J., Jang, H. K., Lim, J. H., Lee, D., Lee, J. H., Bae, H., et al. (2020). Characteristics of different size phytoplankton for primary production and biochemical compositions in the Western East/Japan Sea. *Front. Microbiol.* 11. doi: 10.3389/fmicb.2020.560102

Kang, J. J., Joo, H. T., Lee, J. H., Lee, J. H., Lee, H. W., Lee, D., et al. (2017). Comparison of biochemical compositions of phytoplankton during spring and fall seasons in the northern East/Japan Sea. *Deep. Res. Part II Top. Stud. Oceanogr.* 143, 73-81. doi: 10.1016/j.dsr2.2017.06.006

Keil, R. G., Tsamakis, E., and Hedges, J. I. (2000). "Early diagenesis of particulate amino acids in marine systems," in *Perspectives in amino acid and protein geochemistry* ,(New York: Oxford University Press), pp 69–82.

Kim, K.-R., and Kim, K. (1996). What is happening in the East Sea (Japan sea)?: recent chemical observations during CREAMS 93-96. *J. Korean Soc Oceanogr.* 31, 164–172.

Kim, K., Kim, K. R., Min, D. H., Volkov, Y., Yoon, J. H., and Takematsu, M. (2001). Warming and structural changes in the east (Japan) sea: A clue to future changes in global oceans? *Geophys. Res. Lett.* 28 (17), 3293-3296. doi: 10.1029/2001GL013078

Kim, T. H., Lee, Y. W., and Kim, G. (2010). Hydrographically mediated patterns of photosynthetic pigments in the East/Japan Sea: Low N:P ratios and cyanobacterial dominance. *J. Mar. Syst.* 82, 72–79. doi: 10.1016/j.jmarsys.2010.03.005

Kim, S. W., Saitoh, S. I., Ishizaka, J., Isoda, Y., and Kishino, M. (2000). Temporal and spatial variability of phytoplankton pigment concentrations in the Japan sea derived from CZCS images. *J. Oceanogr.* 56 (5), 527-538. doi: 10.1023/A:1011148910779

Kim, H.c., Yoo, S., and Oh, I. S. (2007). Relationship between phytoplankton bloom and wind stress in the sub-polar frontal area of the Japan/East Sea. *J. Mar. Syst.* 67 (3-4), 205-216. doi: 10.1016/j.jmarsys.2006.05.016

Kim, Y., Youn, S. H., Oh, H. J., Kang, J. J., Lee, J. H., Lee, D., et al. (2020). Spatiotemporal variation in phytoplankton community driven by environmental factors in the northern east china sea. *Water (Switzerland)* 12 (10), 2695. doi: 10.3390/w12102695

Kirk, J. T. O. (1985). Effects of suspensoids (turbidity) on penetration of solar radiation in aquatic ecosystems. *Hydrobiologia* 125 (1), 195-208. doi: 10.1007/BF00045935

Kleppel, G. S., Burkart, C. A., and Houchin, L. (1998). Nutrition and the regulation of egg production in the calanoid copepod acartia tonsa. *Limnol. Oceanogr.* 43 (5), 1000-1007. doi: 10.4319/lo.1998.43.5.1000

Kolmakova, A. A., and Kolmakov, V. I. (2019). Amino acid composition of green microalgae and diatoms, cyanobacteria, and zooplankton (Review). *Inl. Water Biol.* 12, 452–461. doi: 10.1134/S1995082919040060

Konopka, A., and Brock, T. D. (1978). Effect of temperature on blue-green algae (Cyanobacteria) in lake mendota. *Appl. Environ. Microbiol.* 36, (4), 572-576. doi: 10.1128/aem.36.4.572-576.1978

Kremp, A., Godhe, A., Egardt, J., Dupont, S., Suikkanen, S., Casabianca, S., et al. (2012). Intraspecific variability in the response of bloom-forming marine microalgae to changed climate conditions. *Ecol. Evol.* 2, (6), 1195-1207. doi: 10.1002/ece3.245

Kuznetsova, M., Lee, C., Aller, J., and Frew, N. (2004). Enrichment of amino acids in the sea surface microlayer at coastal and open ocean sites in the north Atlantic ocean. *Limnol. Oceanogr.* 49 (5), 1605-1619. doi: 10.4319/lo.2004.49.5.1605

Lønborg, C., Doyle, J., Furnas, M., Menendez, P., Benthuysen, J. A., and Carreira, C. (2017). Seasonal organic matter dynamics in the great barrier reef lagoon: Contribution of carbohydrates and proteins. *Cont. Shelf Res.* 138, 95–105. doi: 10.1016/j.csr.2017.01.010

Lean, D. R. S., and Pick, F. R. (1981). Photosynthetic response of lake plankton to nutrient enrichment: A test for nutrient limitation. *Limnol. Oceanogr.* 26 (6), 1001-1019. doi: 10.4319/lo.1981.26.6.1001

Lee, C., and Cronin, C. (1984). Particulate amino acids in the Sea: Effects of primary productivity and biological decomposition. *J. Mar. Res.* 42, 1075–1097. doi: 10.1357/002224084788520710

Lee, S. H., Joo, H. T., Lee, J. H., Lee, J. H., Kang, J. J. , Lee, H. W., et al. (2017b). Seasonal carbon uptake rates of phytoplankton in the northern East/Japan Sea. *Deep. Res. Part II Top. Stud. Oceanogr.*, 143, 45-53. doi: 10.1016/j.dsr2.2017.04.009

Lee, J. Y., Kang, D. J., Kim, I. N., Rho, T., Lee, T., Kang, C. K., et al. (2009). Spatial and temporal variability in the pelagic ecosystem of the East Sea (Sea of japan): A review. *J. Mar. Syst.* 78, 288-300. doi: 10.1016/j.jmarsys.2009.02.013

Lee, J. H., Lee, D., Kang, J. J., Joo, H. T., Lee, J. H. , Lee, H. W., et al. (2017a). The effects of different environmental factors on the biochemical composition of particulate organic matter in gwangyang bay, south Korea. *Biogeosciences* 14, (7), 1903-1917. doi: 10.5194/bg-14-1903-2017

Lee, S. H., Son, S., Dahms, H. U., Park, J. W., Lim, J. H., Noh, J. H., et al. (2014). Decadal changes of phytoplankton chlorophyll-a in the East Sea/Sea of Japan. *Oceanology* 54 (6), 771-779. doi: 10.1134/S0001437014060058

Lehmann, M. F., Carstens, D., Deek, A., McCarthy, M., Schubert, C. J., and Zopfi, J. (2020). Amino acid and amino sugar compositional changes during *in vitro* degradation of algal organic matter indicate rapid bacterial re-synthesis. *Geochim. Cosmochim. Acta* 283, 67–84. doi: 10.1016/j.gca.2020.05.025

Liebezeit, G., and Bölter, M. (1986). Distribution of particulate amino acids in the bransfield strait. *Polar Biol* 5 (4), 199-206. doi: 10.1007/BF00446087

Lim, S. H., Jang, C. J., Oh, I. S., and Park, J. J. (2012). Climatology of the mixed layer depth in the East/Japan Sea. *J. Mar. Syst.* 96, 1-14. doi: 10.1016/j.jmarsys.2012.01.003

Liu, Z., and Xue, J. (2020). The lability and source of particulate organic matter in the northern gulf of Mexico hypoxic zone. *J. Geophys. Res. Biogeosci.* 125 (9), e2020JG005653 . doi: 10.1029/2020JG005653

Lowry, O. H., Rosebrough, N. J., Farr, A. L., and Randall, R. J. (1951). Protein measurement with the folin phenol reagent. *J. Biol. Chem.* 193, 265-275. doi: 10.1016/0922-338X(96)89160-4

Mackey, M. D., Mackey, D. J., Higgins, H. W., and Wright, S. W. (1996). CHEMTAX - a program for estimating class abundances from chemical markers: Application to HPLC measurements of phytoplankton. *Mar. Ecol. Prog. Ser* 144, 265-283. doi: 10.3354/meps144265

Marsh, J. B., and Weinstein, D. B. (1966). Simple charring method for determination of lipids. *J. Lipid Res* 7 (4), 574-576. doi: 10.1016/S0022-2275(20)39274-9

Mente, E., Coutteau, P., Houlihan, D., Davidson, I., and Sorgeloos, P. (2002). Protein turnover, amino acid profile and amino acid flux in juvenile shrimp litopenaeus vannamei: Effects of dietary protein source. *J. Exp. Biol.* 205, 3107–3122. doi: 10.1242/jeb.205.20.3107

Meyers, P. A. (1994). Preservation of elemental and isotopic source identification of sedimentary organic matter. *Chem. Geol.* 114, 289–302. doi: 10.1016/0009-2541(94)90059-0

Middelburg, J. J., and Herman, P. M. J. (2007). Organic matter processing in tidal estuaries. *Mar. Chem.* 106 (1-2), 127-147. doi: 10.1016/j.marchem.2006.02.007

Montagnes, D. J. S., Berges, J. A., Harrison, P. J., and Taylor, F. J. R. (1994). Estimating carbon, nitrogen, protein, and chlorophyll a from volume in marine phytoplankton. *Limnol. Oceanogr.* 39 (5), 1044-1060. doi: 10.4319/lo.1994.39.5.1044

Morris, I. (1981). Photosynthetic products, physiological state, and phytoplankton growth. Physiological Bases of Phytoplankton Ecology *Can. Bull. Fish. Aquat. Sci.* 210, 83-102.

Morris, I., Glover, H. E., and Yentsch, C. S. (1974). Products of photosynthesis by marine phytoplankton: the effect of environmental factors on the relative rates of protein synthesis. *Mar. Biol.* 27 (1), 1-9. doi: 10.1007/BF00394754

Muller-Navarra, D. (1995). Evidence that a highly unsaturated fatty acid limits daphnia growth in nature. *Arch. Fur Hydrobiol.* 132, 297-307. doi: 10.1127/archiv-hydrobiol/132/1995/297

Oser, B. L. (1959). "An integrated essential amino acid index for predicting the biological value of proteins," in *Protein and amino acid nutrition* (New York: Academic Press), pp. 295-311. doi: 10.1016/b978-0-12-395683-5.50014-6

Padial, A. A., and Thomaz, S. M. (2008). Prediction of the light attenuation coefficient through the secchi disk depth: Empirical modeling in two large Neotropical ecosystems. *Limnology* 9 (2), 143-151. doi: 10.1007/s10201-008-0246-4

Parsons, T. R., Maita, Y., and Lalli, C. M. (1984). A manual of chemical & biological methods for seawater analysis. *Mar. pollut. Bull.* 15, 419–420. doi: 10.1016/0025-326x(84)90262-5

Peters, E. (1996). Prolonged darkness and diatom mortality: II. marine temperate species. *J. Exp. Mar. Bio. Ecol.* 207 (1-2), 43-58. doi: 10.1016/0022-0981(95)02519-7

Piontek, J., Händel, N., Langer, G., Wohlers, J., Riebesell, U., and Engel, A. (2009). Effects of rising temperature on the formation and microbial degradation of marine diatom aggregates. *Aquat. Microb. Ecol.* 54 (3), 305-318. doi: 10.3354/ame01273

Ramette, A. (2007). Multivariate analyses in microbial ecology. *FEMS Microbiol. Ecol.* 62 (2), 142-160. doi: 10.1111/j.1574-6941.2007.00375.x

Ríos, A. F., Fraga, F., Pérez, F. F., and Figueiras, F. G. (1998). Chemical composition of phytoplankton and particulate organic matter in the ría de vigo (NW Spain). *Sci. Mar.* 62 (3), 257-271. doi: 10.3989/scimar.1998.62n3257

Sabadel, A. J. M., Van Oostende, N., Ward, B. B., S.Woodward, E. M., Van Hale, R., and Frew, R. D. (2019). Characterization of particulate organic matter cycling during a summer north Atlantic phytoplankton bloom using amino acid c and n stable isotopes. *Mar. Chem.* 214, 103670. doi: 10.1016/j.marchem.2019.103670

Savoye, N., Aminot, A., Tréguer, P., Fontugne, M., Naulet, N., and Kérouel, R. (2003). Dynamics of particulate organic matter δ15N and δ13C during spring phytoplankton blooms in a macrotidal ecosystem (Bay of seine, France). *Mar. Ecol. Prog. Ser.* 255, 27–41. doi: 10.3354/meps255027

Sheridan, C. C., Lee, C., Wakeham, S. G., and Bishop, J. K. B. (2002). Suspended particle organic composition and cycling in surface and midwaters of the equatorial pacific ocean. *Deep. Res. Part I Oceanogr. Res. Pap.* 49, 1983–2008. doi: 10.1016/S0967-0637(02)00118-8

Shields, M. R., Bianchi, T. S., Osburn, C. L., Kinsey, J. D., Ziervogel, K., Schnetzer, A., et al. (2019). Linking chromophoric organic matter transformation with biomarker indices in a marine phytoplankton growth and degradation experiment. *Mar. Chem.* 214, 103665. doi: 10.1016/j.marchem.2019.103665

ter Braak, C. J. F., and Šmilauer, P. (2002). "CANOCO reference manual and CanoDraw for windows user's guide: Software for canonical community ordination (Version 4.5)," in *Sect. permut. methods* (Ithaca, New York: Microcomput. Power).

Thompson, P. A., Guo, M.-x., and Harrison, P. J. (1992). Effects of variation in temperature. I. On the biochemical composition of eight species of marine phytoplankton. *J. Phycol.* 28 (4), 481-488. doi: 10.1111/j.0022-3646.1992.00481.x

Townsend, D. W., Keller, M. D., Sieracki, M. E., and Ackleson, S. G. (1992). Spring phytoplankton blooms in the absence of vertical water column stratification. *Nature* 360 (6399), 59-62. doi: 10.1038/360059a0

Tsukasaki, A., and Tanoue, E. (2010). Chemical characterization and dynamics of particulate combined amino acids in pacific surface waters. *J. Mar. Syst.* 79, 173–184. doi: 10.1016/j.jmarsys.2009.08.003

Tyson, R. V. (1995). "The nature of organic matter in sediments," in *Sedimentary organic matter.* (Dordrecht: Springer), 7–28.

Unger, D., Ittekkot, V., Schäfer, P., and Tiemann, J. (2005). Biogeochemistry of particulate organic matter from the bay of Bengal as discernible from hydrolysable neutral carbohydrates and amino acids. *Mar. Chem.* 96, 155–184. doi: 10.1016/j.marchem.2004.12.005

Vargas, C. A., Escribano, R., and Poulet, S. (2006). Phytoplankton food quality determines time windows for successful zooplankton reproductive pulses. *Ecology* 87, 2992–2999. doi: 10.1890/0012-9658(2006)87[2992:PFQDTW]2.0.CO;2

Vinogradov, M. E., Shushkina, E. A., and Vedernikov, V. I. (1996). The features of epipelagic ecosystems of the pacific from satellite and expeditionary data. primary production and its seasonal variations. *Oceanology* 36 (2), 222-230.

Wei, Y., Chen, Z., Guo, C., Zhong, Q., Wu, C., and Sun, J. (2020). Physiological and ecological responses of photosynthetic processes to oceanic properties and phytoplankton communities in the oligotrophic Western pacific ocean. *Front. Microbiol.* 11. doi: 10.3389/fmicb.2020.01774

Wie, J., Moon, B. K., Hyun, Y. K., and Lee, J. (2021). Impact of local atmospheric circulation and sea surface temperature of the East Sea (Sea of Japan) on heat waves over the Korean peninsula. *Theor. Appl. Climatol.* 144 (1), 431-446. doi: 10.1007/s00704-021-03546-8

Wu, Y., Dittmar, T., Ludwichowski, K. U., Kattner, G., Zhang, J., Zhu, Z. Y., et al. (2007). Tracing suspended organic nitrogen from the Yangtze river catchment into the East China Sea. *Mar. Chem.* 107, 367–377. doi: 10.1016/j.marchem.2007.01.022

Wu, Y., Liu, Z., Hu, J., Zhu, Z., Liu, S., and Zhang, J. (2016). Seasonal dynamics of particulate organic matter in the changjiang estuary and adjacent coastal waters illustrated by amino acid enantiomers. *J. Mar. Syst.* 154, 57–65. doi: 10.1016/j.jmarsys.2015.04.006

Ye, F., Guo, W., Shi, Z., Jia, G., and Wei, G. (2017). Seasonal dynamics of particulate organic matter and its response to flooding in the pearl river estuary, China, revealed by stable isotope (δ13C and δ15N) analyses. *J. Geophys. Res. Ocean.* 122 (8), 6835-6856. doi: 10.1002/2017JC012931

Yoo, S., and Kim, H. C. (2004). Suppression and enhancement of the spring bloom in the southwestern East Sea/Japan Sea. *Deep. Res. Part II Top. Stud. Oceanogr.* 51 (10-11), 1093-1111. doi: 10.1016/j.dsr2.2003.10.008

Yoo, S., and Park, J. (2009). Why is the southwest the most productive region of the East Sea/Sea of Japan? *J. Mar. Syst.* 78 (2), 301-315. doi: 10.1016/j.jmarsys.2009.02.014

Zapata, M., Rodríguez, F., and Garrido, J. L. (2000). Separation of chlorophylls and carotenoids from marine phytoplankton: A new HPLC method using a reversed phase C8 column and pyridine-containing mobile phases. *Mar. Ecol. Prog. Ser.* 195, 29-45. doi: 10.3354/meps195029

Zhang, P. Y., Yang, G. P., Chen, Y., Leng, W. S., and Ji, C. X. (2016). Temporal and spatial variations of particulate and dissolved amino acids in the East China Sea. *Mar. Chem.* 186, 133–144. doi: 10.1016/j.marchem.2016.09.004

Zhu, Z. Y., Wu, Y., Liu, S. M., Wenger, F., Hu, J., Zhang, J., et al. (2016). Organic carbon flux and particulate organic matter composition in Arctic valley glaciers: Examples from the bayelva river and adjacent kongsfjorden. *Biogeosciences* 13, 975–987. doi: 10.5194/bg-13-975-2016

Zweifel, U. L., Norrman, B., and Hagstrom, A. (1993). Consumption of dissolved organic carbon by marine bacteria and demand for inorganic nutrients. *Mar. Ecol. Prog. Ser.* 101, 23-32. doi: 10.3354/meps101023